



**HAL**  
open science

# Microalgal biofuels: Pathways towards a positive energy balance

Vladimir Heredia, Jack Legrand, Jeremy Pruvost

## ► To cite this version:

Vladimir Heredia, Jack Legrand, Jeremy Pruvost. Microalgal biofuels: Pathways towards a positive energy balance. *Energy Conversion and Management*, 2022, 267, pp.115929. 10.1016/j.enconman.2022.115929 . hal-04209725

**HAL Id: hal-04209725**

**<https://hal.science/hal-04209725>**

Submitted on 18 Sep 2023

**HAL** is a multi-disciplinary open access archive for the deposit and dissemination of scientific research documents, whether they are published or not. The documents may come from teaching and research institutions in France or abroad, or from public or private research centers.

L'archive ouverte pluridisciplinaire **HAL**, est destinée au dépôt et à la diffusion de documents scientifiques de niveau recherche, publiés ou non, émanant des établissements d'enseignement et de recherche français ou étrangers, des laboratoires publics ou privés.

# Microalgal biofuels: Pathways towards a positive energy balance.

Vladimir Heredia<sup>1</sup>, Jack Legrand<sup>1</sup>, and Jeremy Pruvost<sup>1\*</sup>

<sup>1</sup>Nantes Université, Oniris, GEPEA, UMR 6144 F-44600, Saint-Nazaire, France

\*Corresponding author: [jeremy.pruvost@univ-nantes.fr](mailto:jeremy.pruvost@univ-nantes.fr)

Submitted to: Energy Conversion and Management  
June 10, 2022

## Abstract

Current microalgae biofuel production pathways are still far from being energetically self-sufficient. Simulations scenarios (1 t·y<sup>-1</sup> of biomass) under a purely energetic perspective, have revealed some bottlenecks mainly in the cultivation and metabolite recovery processes. Technologies such as intensified photobioreactors such as AlgoFilm©, infrared light filtering units, photovoltaic panels, solvent-free metabolite recovery processes, and high biomass concentration treatments at  $\geq 145 \text{ kg}\cdot\text{m}^{-3}$  are suggested and discussed to also have a major contribution on the net energy ratio of the process. An energy-driven biorefinery approach has been proposed to increase the energy output by obtaining bioethanol and biodiesel liquid fuels, but also photovoltaic energy during the same production process. The latter may also compensate for the large amounts of energy consumed in typical operations of the wet-pathway processes like harvesting-concentration, cell disruption, or solvent recycling processes. This perspective increased the final volume of liquid biofuels up to 57%. It was found a maximum net energy ratio of 1.9 for a double biofuel process, and 8.5 if photovoltaic energy is also considered.

---

*Keywords: Biofuels; Biorefinery; Photobioreactor; Net Energy ratio; Process simulation*

---

## 18 **1 Introduction**

19 Energy-efficient fuel processes are crucial for the sustainable transport industry. During the last  
20 decades, biofuels from microalgae have been shown as an alternative for supplying the ever-growing  
21 energy demand of liquid biofuels while contributing to the CO<sub>2</sub> emissions decrease [1–6]. Similarly,  
22 it has been demonstrated that microalgae-based biofuels can be produced while treating wastewater,  
23 which increases the environmental impact of the production process [7–9]. However, microalgae-  
24 based processes are still challenging in terms of sustainability, economics, and energy efficiency  
25 for large-scale implementation [10–12]. The accumulation of energy-rich metabolites in the cell,  
26 and the chosen process to produce, recover and transform such molecules into biofuels is key for  
27 recovering the maximum of energy from microalgae biomass while investing a minimum of energy  
28 during the processing.

29 The first challenge is to increase the productivity of strains with large content of energy-rich  
30 metabolites during the cultivation stage. Several works have described culturing protocols and  
31 screening systems to choose the most interesting strain with high metabolite contents [13–18]. For  
32 example, *Parachlorella kessleri* (freshwater species) and *Nannochloropsis gaditana* (marine species)  
33 have been described to accumulate triacylglycerol TAG, both up to 24%<sub>X</sub>; and 64%<sub>X</sub> and 23%<sub>X</sub>  
34 carbohydrates respectively under nitrogen limitation, chemostat mode and continuous light [19, 20].  
35 In comparison, *N. gaditana* has also accumulated TAG up to 40%<sub>X</sub> during batch nitrogen-depleted  
36 cultivation [21, 22]. Important attention has also to be paid to the conception and operation of  
37 the photobioreactor systems to produce microalgae biomass[23, 24]. Process intensification is an  
38 approach that takes advantage of dimension optimization to create more energy-efficient process  
39 technologies [25]. Such a concept can be applied to microalgal culture systems, leading to high  
40 volumetric productivity photobioreactors (HVP PBRs). Increasing the specific illuminated surface  
41 is translated into a culture depth reduction. Thus, volumetric productivity, as well as biomass  
42 concentration, are increased for a given light supply, and then surface productivity. As shown in  
43 Pruvost et al. [26] and Legrand [27], introducing thin-film PBR can lead to a volume reduction of one  
44 or two orders of magnitude for a given biomass production when compared to usual culture systems  
45 with depths in the usual range of 0.05 - 0.15 m. For the energy investment during the biomass  
46 production stage, Nwoba et al. [28] recently reported an alternative to reduce the energy input by

47 using a flat panel photobioreactor constructed of insulated-glazed units (IGUs, for Infrared light  
48 filtering) with an integrated energy-generating photovoltaic (PV) panel. With this technology,  
49 it is argued to isolate the microalgae culture of >90% of the ultraviolet and infrared spectral  
50 components, while still letting pass >75% of visible light. As a result, the energy needs for thermal  
51 regulation are strongly reduced while simultaneously producing electricity from the PV panel.

52 Once larger amounts of energy-rich metabolites are produced in photobioreactors PBR, they  
53 need to be recovered and converted into biofuels: TAG into BioDiesel, and carbohydrates into  
54 bioethanol. One of the first approaches to do so was the dry pathway in biodiesel production.  
55 After harvesting and drying the biomass during the culture stage, TAG molecules are recovered via  
56 solid-liquid extraction. However, this process invests large amounts of energy for heating and to  
57 facilitate extraction, and solvent recycling. This may strongly impact the global energy efficiency  
58 by investing more energy than the potentially recoverable [29, 30].

59 An alternative approach is the wet-pathway. It considers the release of all the intracellular  
60 material into the bulk medium through cell disruption, and then the recovery of the energy-rich  
61 metabolites from the liquid phase (liquid-liquid extraction). This process has been shown to reduce  
62 energy consumption by the avoidance of around  $17.71 \text{ MJ} \cdot \text{kg}_{Biomass}^{-1}$  used during the drying process  
63 of the dry-pathway [31].

64 There exist several methods that may be applied for the cell disruption stage during a wet  
65 pathway process [32]. Safi et al. [33] and Lee et al. [34] compared several methods regarding  
66 energy consumption. They concluded that bead-milling processes required less intensive operating  
67 conditions (like operating time or pressure) which impacts directly the energy cost of the operation.  
68 Bead milling was already proved efficient for microalgal biomass [35–37]

69 The recovery of the released TAG after cell disruption is based on the affinity to different solvents  
70 during the liquid-liquid extraction (considering the TAG as a hydrophobic compound). Several  
71 methods have been studied on this matter [10, 38, 39, 30] and it is considered that lipid extraction  
72 after cell disruption is still a bottleneck in the biodiesel production process. The chosen method is  
73 expected to be energy efficient but also to optimize the extraction of targeted compounds (ideally  
74 TAG) while being sufficiently metabolite-selective to minimize the purification steps before final  
75 biodiesel conversion [30]. Harris et al. [40] has pointed out the benefits of using wet biomass during  
76 the extraction, mainly regarding again the energy-saving by the avoidance of drying biomass. It also

77 suggested the interest in intensified processes, which will enhance the economic and environmental  
78 impacts of the process. Regarding intensified operations, the centrifugal extraction technologies  
79 (as continuous centrifugal extraction CCE) combined with the appropriate solvent choice arises as  
80 a promising technology capable of simultaneously performing extraction and separation operations  
81 [41–43]. However, some parameters such as biomass concentration, solvent choice, or feeding flow  
82 rates may promote emulsification phenomena which would reduce the operating work-zone and  
83 extraction yield of the process [44]. It is important to note that centrifugal extraction technologies  
84 also enable the separation and recovery of the available carbohydrates in the non-extracted phase  
85 [45] for concomitant bioethanol production.

86 An interesting strategy to optimize the biofuel process is to maximize the energy output by lead-  
87 ing an energy-driven biorefinery approach. So far, the biorefinery is considered one of the strategies  
88 to exploit the highest value of microalgal cultures. Even though, biorefinery is mainly proposed as  
89 a strategy to recover by-products for other market fields (*eg.* nutraceuticals or cosmetics)[46–48],  
90 it could also be applied to energy valorization [49]. Some authors have argued that the only way  
91 to improve the economic or life-cycle analysis of solely liquid biofuels production (often only for  
92 biodiesel) is by the valorization of by-products/co-products [50–52]. As part of this approach, a  
93 double recovery of energy reserve molecules (lipids and carbohydrates) towards the conversion into  
94 two liquid biofuels (bioethanol and biodiesel) is proposed in this work.

95 Yuan et al. [31] showed a net energy ratio  $<1$  for BioDiesel only, implying that the chosen  
96 production system is not capable of producing more energy than it consumes. In this last study,  
97 cultivation and oil extraction dominated energy consumption. Likewise, according to Sander and  
98 Murthy [53], for each 24 kg (28 L, 1 GJ of energy) of algal BioDiesel, 34 kg of byproducts are  
99 produced. If a cellulose-to-ethanol yield of 85% was assumed on the byproducts, it may result  
100 in an additional 6.28 L of ethanol. Borowitzka and Moheimani [54] also argued that an average  
101 yield of 0.13 L bioethanol per kg of algal biomass and 0.12 L biodiesel per kg of algae biomass,  
102 may appear to be reasonable for biofuel valorization. Harun et al. [55], Karemore and Sen [56]  
103 and Sivaramakrishnan and Incharoensakdi [57] have shown the viability of the double liquid biofuel  
104 production at lab scale. They yielded  $4\text{--}6\text{ kg}\cdot\text{m}^{-3}$  of ethanol during the fermentation of lipid-  
105 extracted and hydrolyzed microalgae biomass. By itself, the bioethanol production process from  
106 microalgae manifested a net energy ratio of 0.45 with an energy consumption of  $2\,749.6\text{ GJ}\cdot\text{y}^{-1}$

107 (for 200 t·y<sup>-1</sup> biomass production) according to Hossain et al. [58].

108 Based on the above, the purpose of this work is to simulate the conjunction of particular emerg-  
109 ing technologies (from culture to metabolite recovery process only) for microalgae-based biofuels  
110 production under an energy-driven biorefinery approach and to evaluate the impact on the pro-  
111 cess energy efficiency only (Techno-economical and Life Cycle Assessments are out of the scope of  
112 this work). The simulations will be mainly focused on biodiesel production with the supplement-  
113 tal inclusion of photovoltaic and bioethanol as secondary energy outputs issued from microalgae  
114 cultivation.

## 115 **2 Materials and Methods**

### 116 **2.1 General process description and system boundaries**

117 An algorithm sequence in Excel (Microsoft, USA) has been used to simulate the biofuel production  
118 process. Four operation blocks (each with its corresponding operation units) have been organized  
119 (Fig. 1) for biomass production (Prod-100), metabolite recovery (Rec-200), and biodiesel (BioD-  
120 300) and bioethanol conversions (BioE-400). Each operation block includes operation units or tech-  
121 nologies that may differ for each simulated case (see further details in section 2.4). The biomass  
122 production block includes the photobioreactor (PBR-101) and concentration operations (centrifuga-  
123 tion C-102, flotation Fl-102, band filtration F-102, or none). Metabolite recovery block includes  
124 pretreatment operations (thermal dryer TD-201 or bead milling BM-201) and lipid recovery units  
125 (solid-liquid extraction DX-202, centrifugal liquid-liquid extraction CX-202, or decantation Dec-  
126 202). The biodiesel conversion block comprises extraction solvent recovery by evaporation (D-301),  
127 transesterification in a stirred tank reactor STR (R-302) and biodiesel purification (D-302). The  
128 bioethanol conversion block considers the fermentation in a stirred tank reactor STR (R-401) and  
129 ethanol purification (D-402) units.

130 The system only considers four general mass inputs streams (S) which directly participate in  
131 energy conversion: culture medium and initial inoculum (S-101) for biomass growth, lipid extraction  
132 solvent (S-203) to recover energy-rich molecules, methanol Me-OH for transesterification (S-303)  
133 and water dilution streams (S-202 and S-401) to adjust concentrations in the process. It also  
134 considers three mass outputs: biodiesel (S-305), bioethanol (S-403), and general waste streams.

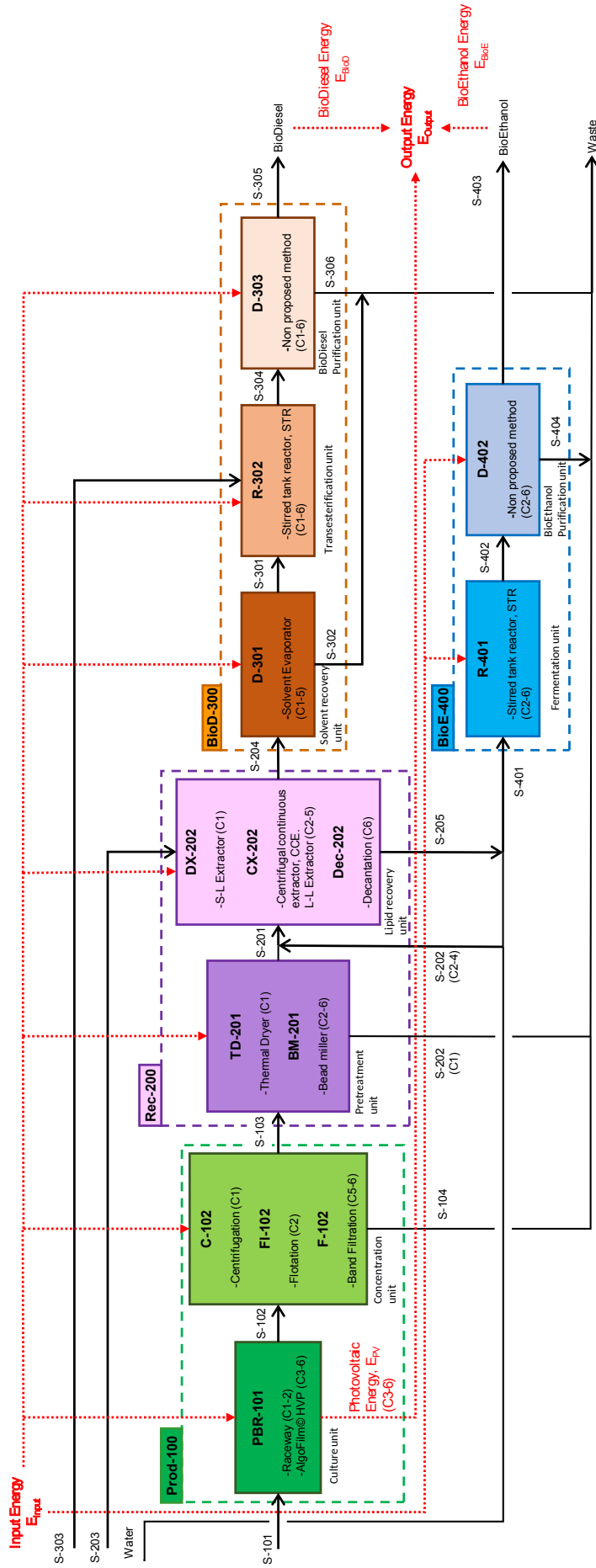


Figure 1: Process flowchart for a microalgae-based biofuel production based on the energy-driven biorefinery approach. Red-dotted lines represent the energy input/output and black-continuous lines the mass flow between operation units. Dashed lines (in four different colors) encompass the four operation blocks described in Section 2.1. Note that the use of operations TD-201 (thermal drying) and DX-202 (S-L extraction) define the dry-pathway process, and the rest of operations are used for the wet-pathway process.

135 Similarly, energy outputs were only photovoltaic Energy ( $E_{PV}$ ) and energies from biodiesel and  
136 bioethanol ( $E_{BioD}$  and  $E_{BioE}$  respectively). This work is focused on global energy consumption  
137 and, as consequence the only energy inputs considered were those related to electricity consumption  
138 at each operation unit. Further details about the specific values and calculations for each operation  
139 unit are detailed in section 2.2.

140 Energy inputs like embodied energies, labor, pumping, inoculum and medium production, plant  
141 deconstruction, and other maintenance sub-operations were not considered here. Some of the  
142 latter may add information not related to the net energy process within the scope of this energy  
143 balance since they depend on the logistics and infrastructure of a given installation when the main  
144 operations units of the process do remain the same. Therefore, the energy costs related to the  
145 mentioned aspects will not be considered in this work.

146 The two main biofuel production pathways have been simulated: the dry-pathway and the  
147 wet-pathway. Simulations were conducted for  $1 \text{ t}\cdot\text{y}^{-1}$  of dried biomass and operating process time  
148 ( $t_{OP}$ ) of 365 d. The simulated production process can be described as follows:

- 149 1) First, biomass is grown in PBR-101 using S-101 as mass input. Main equipment description,  
150 protocols, and strains according to each simulation case are described in Table 1. For PBR-  
151 101, the only energy input was due to electric consumption for culture mixing. Photovoltaic  
152 co-production (PV) may be considered in the energy output for some scenarios.
- 153 2) Next biomass is harvested and may be concentrated using C-102, Fl-102, or F-102. The  
154 mass outputs, S-103 and S-104, go to the Rec-200 block and to the general waste stream  
155 respectively. For the wet-pathway scenarios, the collected biomass in S-103 passes into a  
156 storage tank to be further batched at the first pretreatment unit. Ever since the following  
157 operations units were considered also as batch processes in wet-pathway scenarios only.
- 158 3) For the dry-pathway, the TD-201 unit dries the harvested biomass in S-103 for obtaining  
159 the S-201 stream (dry biomass) and the S-202 (with the evaporated water to waste). For  
160 the wet-pathway, a batched stream with harvested biomass from the storage tank (usually  
161 referred to here as S-103a) is treated by the BM-201, which will disrupt it and release all the  
162 cellular content in the S-201 stream. Process output S-201 is then directed to lipid recovery  
163 units (DX-202, CX-202, or Dec-202).

164 4) In the dry-pathway, non-released lipids (still intracellular lipids) in the stream S-201 are  
165 extracted using n-hexane Hex (S-203) using the solid-liquid extraction unit DX-202. The  
166 mixture of solvent and lipids go to the BioD-300 block via the S-204 stream, while residual  
167 dried cells are disposed to the general waste stream via the S-205 stream.

168 For the wet-pathway, a S-201a stream may be supposed for the dilution of S-201 with the S-202  
169 stream (water) just before the centrifugal liquid-liquid extraction equipment CX-202. Then,  
170 for the lipid extraction, 2-methyl-tetra-hydrofuran Me-THF (S-203) is used. By centrifuge  
171 force action, two outputs are recovered: S-204 and S-205. The stream S-204 (with the mixture  
172 of solvent and lipids only) is conducted to the BioD-300 block.

173 A non-solvent process for the wet-pathway has been also proposed for lipid recovery. The  
174 decantation operation Dec-202 takes as well the S-201 stream (wet-disrupted biomass) to  
175 obtain the S-204 stream charged with lipids.

176 No matter the option chosen to simulate the lipid extraction unit, the stream S-205 (with  
177 the rest of the polar components, carbohydrates included, and the non-extracted lipids) is  
178 directed to either the general waste stream or the BioE-400 block in case of double biofuel  
179 recovery.

180 5) In the BioD-300 block, lipids molecules are separated first from the extraction solvent using  
181 the D-301 unit. The content of the S-301 stream is then considered to be entirely composed  
182 of lipid molecules heading towards R-302, while the content of S-302, is only composed of  
183 extraction solvent going to the general waste stream.

184 6) Next, the transesterification reaction takes place in R-302 using the lipid molecules (more  
185 precisely triacylglycerol TAG molecules) and the Me-OH required for the reaction (S-301 and  
186 the S-303 respectively). After the reaction, the resultant compounds go to D-303 for the final  
187 recovery.

188 7) The biodiesel final treatment occurs in the D-303 unit. No particular technology has been  
189 proposed for this operation. The fatty acid methyl esters FAME's (biodiesel) produced during  
190 the transesterification of TAG molecules are separated from the reaction residuals or non-  
191 reactant compounds (*eg.* Me-OH, glycerol, fatty acids). The latter are collected in the S-306

192 stream and the biodiesel in the S-305.

193 8) In case of double biofuel recovery, the output stream S-205 (containing polar components and  
 194 carbohydrates) may be diluted to constitute the S-401 stream, and then used as input of the  
 195 R-401 unit at the BioE-400 block. The output S-402 directs the produced bioethanol to the  
 196 D-402 purification unit

197 9) Similarly, at the D-402 bioethanol purification unit, no particular technology has been pro-  
 198 posed for the operation. Fermentation subproducts (*eg.* glycerol, residual carbohydrates,  
 199 enzymes, water) are part of the S-404 stream and go to the general waste stream, while the  
 200 refined bioethanol is recovered in the S-403 stream.

201 To note that the general waste stream (composed of S-104, S-202 of case 1, S-302, S-306, and S-  
 202 404) was not considered a municipal discharge but it only helps to elucidate the amount of discarded  
 203 mass outputs at each cycle of processing.

## 204 2.2 Input calculations

### 205 2.2.1 Streams balance, S

$M_{i,j}$  refers to the mass flow rate of the species  $i$  in the stream  $j$  (if indicated). For all the streams,  
 the total mass flow rate ( $M_T$ ,  $\text{kg}\cdot\text{d}^{-1}$ ) were calculated as:

$$M_T = M_X + M_W + M_S + M_{Me-OH} + M_{BioD} + M_{BioE} + M_Z \quad (1)$$

$$M_X = M_{TAG} + M_{Sg} + M_{XR} \quad (2)$$

206  $M_W$  is for water,  $M_S$  for extraction solvent,  $M_{Me-OH}$  for Me-OH,  $M_{BioD}$  for biodiesel,  $M_{BioE}$  for  
 207 bioethanol,  $M_Z$  for waste (any other residual compound) and  $M_X$  for biomass. The latter divided  
 208 in sub-fractions of TAG ( $M_{TAG}$ ), carbohydrates ( $M_{Sg}$ ) and residual biomass ( $M_{XR}$ ).

209 Volumetric flow rates ( $Q_j$ ,  $\text{m}^3\cdot\text{d}^{-1}$ ) were dependent on the composition of a stream  $j$  and will  
 210 be described below for the corresponding operation unit.

Table 1: Upstream operations syththesis for each simulated Case.

Case	1, 2 & 2.a.	3 & 3.a., 5, 6	4
<b>-Photobioreactor Technology</b>	Raceway	HVP+IGU	HVP+IGU
<b>-Photovoltaic production</b>	no	yes	yes
<b>-Illuminated surface</b>			
$A^*$ (m <sup>2</sup> )	166	166	185
<b>-Operative Volume</b>			
$V_O$ (m <sup>3</sup> )	25	0.33	0.37
<b>-Specific Illuminated surface</b>			
$a_s$ (m <sup>-1</sup> )	6.67	500	500
<b>-PBR Depth</b>			
$L$ (m)	0.150	0.002	0.002
<b>-Strain</b>	Ideal Strain <sup>†</sup>	Ideal Strain <sup>†</sup>	<i>N. gaditana</i> <sup>††</sup>
<b>-Surface Productivity</b>			
$S_X$ ( $\cdot 10^{-3}$ kg $\cdot$ m <sup>-2</sup> $\cdot$ d <sup>-1</sup> )	16.5 <sup>†</sup>	16.5 <sup>†</sup>	14.9 <sup>††</sup>
<b>-Dilution rate</b>			
$D$ (h <sup>-1</sup> )	0.036 <sup>†</sup>	0.036 <sup>†</sup>	0.01 <sup>††</sup>
<b>-TAG content</b>			
% <sub>X</sub> TAG	36 <sup>†††</sup>	36 <sup>†††</sup>	15 <sup>††</sup>
<b>-Carbohydrates content</b>			
% <sub>X</sub> Sg	40 <sup>†††</sup>	40 <sup>†††</sup>	23 <sup>††</sup>
<b>-Potentially Recoverable biodiesel energy</b>			
$E_{P,BioD}$ (MJ $\cdot$ t <sup>-1</sup> $\cdot$ y <sup>-1</sup> )	14 196	14 196	5 836
<b>-Potentially Recoverable bioethanol energy</b>			
$E_{P,BioE}$ (MJ $\cdot$ t <sup>-1</sup> $\cdot$ y <sup>-1</sup> )	5 447	5 447	3 132
<b>-Potentially Recoverable BioFuel energy</b>			
$E_P$ (MJ $\cdot$ t <sup>-1</sup> $\cdot$ y <sup>-1</sup> )	19 642	19 642	8 968

<sup>†</sup>Pruvost et al. [24], <sup>††</sup>Heredia et al. [19], <sup>†††</sup>Proposed

HVP+IGU: High Volumetric Productivity Photobioreactor with an Insulated-Glazed Unit

### 211 2.2.2 Culture unit: PBR-101

To compare ideal strain simulations to the one using experimental values (C4), all the other cultures simulated were also assumed to be in continuous mode. Inputs values may be surface productivity,  $S_X$  ( $\text{kg}\cdot\text{m}^{-2}\cdot\text{d}^{-1}$ ); TAG and carbohydrate contents as fraction of the dry biomass concentration ( $\%_X\text{TAG}$  and  $\%_X\text{Sg}$  respectively); dilution rate,  $D$  ( $\text{h}^{-1}$ ); and specific illuminated surface,  $a_s$  ( $\text{m}^{-1}$ ). The S-101 volumetric flow rate ( $Q_{S101}$ ) was consider so that the  $M_{X,102}$  at S-102 reaches the  $1 \text{ t}\cdot\text{d}^{-1}$ . Then, by using the  $Q_{S101}$  the following equations were calculated:

$$Q_{S101} = Q_{S102} \quad (3)$$

$$P_X = S_X \cdot a_s \quad (4)$$

$$X_{S102} = S_X \cdot a_s / D \quad (5)$$

$$L = 1/a_s \quad (6)$$

$$V_{Op} = Q_{S101}/D \quad (7)$$

$$A^* = V_O/L \quad (8)$$

212 where  $P_X$  is for biomass volumetric productivity ( $\text{kg}\cdot\text{m}^{-3}\cdot\text{d}^{-1}$ ),  $V_{Op}$  is the culture operating volume  
213 ( $\text{m}^3$ ),  $A^*$  is the illuminated surface ( $\text{m}^2$ ) and  $X$  is the dry biomass concentration ( $\text{kg}\cdot\text{m}^{-3}$ ).

214 Mixing energy of  $0.368 \text{ kWh}\cdot\text{m}^{-3}\cdot\text{d}^{-1}$  was considered for the raceway culture system, as a result  
215 of mechanical (paddle) agitation and which is close to the values found in the literature [59, 60].  
216 For the high volumetric productivity photobioreactor HVP, it was considered a pneumatic (air  
217 injection) agitation leading to  $1.0 \text{ kWh}\cdot\text{m}^{-3}\cdot\text{d}^{-1}$  [61]. It must be noticed that energy for mixing  
218 could be further refined, for example by using a pump to circulate the culture in technology such  
219 as AlgoFilm<sup>©</sup> PBR. But the influence on results remains moderate because of the large decrease in  
220 volume which in turn reduced the impact of energy requested for mixing (here expressed per unit  
221 of culture volume). Different values for both technologies were however retained to illustrate the  
222 impact of the technical solution to circulate the culture (pneumatic vs mechanical). This aspect  
223 will be discussed in section 3.1.

The energy input of the operation  $E_{Input,PBR101}$  is then related to the culture operating volume

$V_{Op}$  ( $m^3$ ) and to the operating process time  $t_{OP}$ , as detailed here:

$$E_{Input,PBR101} = P_{El,PBR101} \cdot V_O \cdot t_{OP} \quad (9)$$

### 2.2.3 Concentration unit: C-102, Fl-102 and F-102

The technology chosen for the continuous concentration operation depended on the simulation case, however, the calculation set was the same for all of the cases. As an example for the centrifugation operation C-102, the mass balance inputs were the volumetric and mass flow rates of the stream S-102 ( $Q_{S102}$  and  $M_{X,102}$ ), as well as equipment efficiency ( $\eta_{C102}$ ) and moisture percentage for the output ( $\%_{W,C102}$ , w/w). Then, such process would be calculated as follows:

$$Q_{103} = M_{T,103} / \rho_W \quad (10)$$

$$M_{X,103} = M_{X,102} \cdot \eta_{C102} \quad (11)$$

$$M_{W,103} = M_{X,103} \cdot (\%_{W,C102} / (1 - \%_{W,C102})) \quad (12)$$

where  $\rho_W$  (water density,  $1000 \text{ kg}\cdot\text{m}^{-3}$ ) was considered as an average density for the whole culture broth [62].

Total energy input also depended on the technology used. For this operation it was determined from:

$$E_{Input,C102} = Q_{103} \cdot P_{El} \cdot t_{OP} \quad (13)$$

The value  $P_{El}$  was of  $8 \text{ kWh}\cdot\text{m}^{-3}$  for centrifugation [63],  $0.021 \text{ kWh}\cdot\text{m}^{-3}$  for flottation (which was estimated from Zhang and Zhang [64], Xu et al. [65] with values ranged between 0.015 and 0.46  $\text{kWh}\cdot\text{m}^{-3}$ ) and  $0.55 \text{ kWh}\cdot\text{m}^{-3}$  for band filtration [63].

### 2.2.4 Pre-treatment units: TD-201 and BM-201

The pre-treatment unit was simulated considering the harvested biomass in S-103, which was further processed by either thermal drying TD-201 or bead milling BM-201 units according to the corresponding simulation case. The BM-201 process is considered an intermediate storage tank

234 for daily batch treatment.

The mass balance for the TD-201 unit was calculated as follows:

$$Q_{201} = M_{T,201}/\rho_W \quad (14)$$

$$M_{X,201} = M_{X,103} \quad (15)$$

$$M_{W,201} = M_{X,201} \cdot ((1 - \%_{DW,TD201})/\%_{DW,TD201}) \quad (16)$$

235 where the dry biomass percentage for the S-201 output is represented by  $\%_{DW,TD102}$  (w/w) and  
236 the water density  $\rho_W$  was considered as an average density for the biomass.

The energy input for the TD-201 unit was calculated based only on the specific latent heat of vaporization for water ( $\Delta H_{vap,W}$  2 256.8 kJ·kg<sup>-1</sup>). The TD-201 unit was computed as follows:

$$E_{Input,TD-201} = \Delta H_{vap,W} \cdot M_{S,202} \cdot t_{OP} \quad (17)$$

237 where  $t_{OP}$  is the operating full process time described in Section 2.1.

For the mass balance of the BM-201 unit it can be assumed that the S-103 must be processed in a day, it can be assumed equal to the storage tank volume  $V_{Op,Tank}$  (m<sup>3</sup>). Therefore, the operating time for the BM-201  $t_{Op,BM201}$ , takes into account  $V_{Op,Tank}$ , the theoretical stream going out from the intermediate storage tank  $Q_{103a}$  and the number of equipment needed to process it,  $N_{OEq,BM201}$ . This relation is represented in the following equations:

$$Q_{103} = V_{Op,Tank} \quad (18)$$

$$Q_{103a} = V_{eff,BM201}/t_D \quad (19)$$

$$Q_{201} = M_{T,201}/\rho_W \quad (20)$$

$$M_{X,201} = M_{X,103} \quad (21)$$

$$M_{W,201} = M_{W,103} \quad (22)$$

$$V_{eff,BM201} = V_{BM201} \cdot T_{ff} \quad (23)$$

$$t_{Op,BM201} = V_{Op,Tank}/(Q_{103a} \cdot N_{OEq,BM201}) \quad (24)$$

238 where  $t_D$  is the disruption residence time (d) with value of 0.004 d (0.097 h) taken from Heredia

239 et al. [44] for *N. gaditana*, ranging from 10 to 30 kg·m<sup>-3</sup> dry biomass concentration, and achieving  
 240 around 80% disruption rate ( $\tau_D$ ).  $V_{eff,BM201}$  is the effective grinding chamber volume ( $8 \cdot 10^{-3}$  m<sup>3</sup>)  
 241 for a particular bead-milling device with nominal grinding chamber volume  $V_{BM201}$  ( $10 \cdot 10^{-3}$  m<sup>3</sup>)  
 242 and filled percentage value  $T_{ff}$  (80%) according to Zinkoné et al. [36]. The water density  $\rho_W$  was  
 243 considered as an average density for the biomass.

The energy consumption for BM-201 was computed using  $P_{El,BM201}$  of 1.2 kWh·kg<sub>DW</sub><sup>-1</sup> determined by Zinkoné [66]. Calculations were then established as follows:

$$E_{Input,BM201} = P_{El,BM201} \cdot t_{Op,BM201} \quad (25)$$

244 where  $t_{OP}$  is the operating full process time described in Section 2.1.

### 245 2.2.5 Lipid recovery units: DX-202, CX-202 and Dec-202

In the dry-pathway lipids are recovered using the solid-liquid extraction unit DX-202. Mass balance for this operation was calculated as follows:

$$Q_{203} = S/F \cdot Q_{201} \quad (26)$$

$$M_{S,203} = Q_{203} \cdot \rho_{Hex} \quad (27)$$

$$M_{S,204} = M_{S,203} \quad (28)$$

$$M_{TAG,204} = M_{TAG,201} \cdot \eta_{E,TAG} \quad (29)$$

246 where  $S/F$  is solvent to feed inlet ratio with a value of 20 for a TAG extraction efficiency  $\eta_{E,TAG}$   
 247 of 90% according to Delrue et al. [63]; and  $\rho_{Hex}$  is the n-hexane density (659 kg·m<sup>-3</sup> by Kim et al.  
 248 [67]).

The energy input for DX-202, considers the heat demand value  $P_{Q,DX202}$  of 1.74 kWh·kg<sub>DW</sub><sup>-1</sup>, and the electricity demand  $P_{El,DX202}$  of 4.5·10<sup>-4</sup> kWh·kg<sub>DW</sub><sup>-1</sup> according to Delrue et al. [63]. The

resulting calculations were:

$$E_{Q,DX202} = M_{X,201} \cdot P_{Q,DX202} \cdot t_{OP} \quad (30)$$

$$E_{El,DX202} = M_{X,201} \cdot P_{El,DX202} \cdot t_{OP} \quad (31)$$

$$E_{Input,DX202} = E_{Q,DX202} + E_{El,DX202} \quad (32)$$

249 where  $t_{OP}$ ) is the operating full process time described in Section 2.1.

In the wet-pathway, lipids are recovered using either the centrifugal liquid-liquid extraction CX-202 or the decantation Dec-202 units. For the CX-202 unit, mass input values are from the optimized protocol from Heredia et al. [44]. The process may need to consider the dilution of the S-201 stream (to achieve  $7.9 \text{ kg} \cdot \text{m}^{-3}$  in biomass concentration) for obtaining 84% of TAG extraction efficiency  $\eta_{E,TAG}$  using an optimal solvent to feed inlet ratio ( $S/F$ ) of 1.65. With the latter, it is calculated the amount of solvent Me-THF to be used in the S-203. The calculations describing this operation unit were:

$$ToT = Q_{203} + Q_{201a} \leftrightarrow Q_{204} + Q_{205} \quad (33)$$

$$Q_{203} = S/F \cdot Q_{201a} \quad (34)$$

$$M_{TAG,204} = M_{TAG,201a} \cdot \eta_{E,TAG} \cdot \tau_D \quad (35)$$

$$M_{Sg,205} = M_{Sg,201a} \quad (36)$$

250 where the stream S-201a is the dilution of S-201, and  $\tau_D$  corresponds to the disruption rate achieved  
251 in BM-201 (80%, Heredia et al. [44]).

The process was considered to not create emulsions, and so streams S-204 and S-205 will only contain TAG and cell debris (carbohydrates included) respectively.  $ToT$  is the total flow supplied and determines the size and power  $P_{El,CX202}$  of the centrifugal extractor (0.025 kW, Rousselet Robatel, France). Then, the energy consumption for the CX-202 unit is calculated as follows:

$$E_{Input,CX202} = P_{El,CX202} \cdot t_{OP} \quad (37)$$

252 where  $t_{OP}$  is the operating full process time described in Section 2.1.

For the Dec-202 unit, the mass balance has been computed using the following equations:

$$Q_{201} = M_{T,201} / \rho_{AlgLip} \quad (38)$$

$$M_{TAG,204} = M_{TAG,201} \cdot \eta_{E,TAG} \cdot \tau_D \quad (39)$$

$$M_{Sg,205} = M_{TAG,201} \quad (40)$$

$$M_{Sg,205} = M_{Sg,201} \quad (41)$$

253 where  $\tau_D$  corresponds to the disruption rate achieved in BM-201 (80%),  $\eta_{E,TAG}$  is the TAG extrac-  
 254 tion efficiency (here assumed in 95%), and  $\rho_{AlgLip}$  is for the density of algal lipids (1 060 kg·m<sup>-3</sup>,  
 255 Miao and Wu [68]).

The energy input for the Dec-202 operation  $E_{Input,Dec202}$  was defined as follows:

$$E_{Input,Dec202} = P_{El,Dec202} \cdot Q_{201} \cdot t_{OP} \quad (42)$$

256 where  $P_{El,Dec202}$  is the energy demand for the operation established at 0.01 kWh·m<sup>-3</sup> by Zhang  
 257 and Zhang [64], and  $t_{OP}$  is the operating full process time described in Section 2.1.

### 258 2.2.6 Solvent Recovery unit: D-301

If some solvent has been used during the lipid recovery process, it has to be recovered by the solvent recovery unit D-301. The simulation considers a perfect separation of the components by evaporation. Therefore it is assumed:

$$M_{TAG,204} = M_{TAG,301} \quad (43)$$

$$M_{S,302} = M_{S,204} \quad (44)$$

For energy consumption calculation it was only assumed the theoretical latent heat required for phase change:

$$E_{Input,D301} = \Delta H_{vap} \cdot M_{S,204} \cdot t_{OP} \quad (45)$$

259 with  $\Delta H_{vap}$  as the specific latent heat of vaporization (for Me-THF is 375 kJ·kg<sub>MeTHF</sub><sup>-1</sup> taken from

260 Sicaire et al. [69] and for n-hexane is  $360 \text{ kJ}\cdot\text{kg}_{Hex}^{-1}$  taken from Pashchenko and Kuznetsova [70]),  
 261 and  $t_{OP}$  the operating full process time described in Section 2.1.

### 262 **2.2.7 Transesterification unit: R-302**

Conversion of TAG into fatty acid methyl esters (FAME, biodiesel) takes place in the stirred reactor R-302. The process is described by the following equations:

$$M_{BioD,304} = (M_{TAG,301}/MW_{AlgLip}) \cdot 3 \cdot Y_{Trans} \cdot MW_{FAME} \quad (46)$$

$$M_{T,303} = (M_{TAG,301}/MW_{AlgLip}) \cdot (Me-OH/TAG) \cdot MW_{Me-OH} \quad (47)$$

263 where  $MW_{AlgLip}$  is the molecular weight of algal lipids, FAME or Me-OH (920, 299.32, 32.04  
 264  $\text{g}\cdot\text{mol}^{-1}$  respectively) based on Faried et al. [29].

265 The value of 3 in the first equation, represents the stoichiometric coefficient of FAME products  
 266 during transesterification. It has been shown that high transesterification yields  $Y_{Trans}$  may only  
 267 be achieved when using a 6 or 12 Me-OH-to-TAG-moles ratio ( $Me-OH/TAG$ ) [71, 29]. For this  
 268 work, it has been used a ratio of 6  $Me-OH/TAG$  yields 98% conversion in the reaction.

For the calculation of energy consumption, the work of Batan et al. [72] has been used as a reference. The author has reported specific energies for stirring and heating based on the amount of biodiesel produced, leading to:

$$E_{Input,R302} = (P_{El,R302} + P_{Q,R302}) \cdot M_{BioD,304} \quad (48)$$

269 with  $P_{El,R302}$  and  $P_{Q,R302}$  for the specific energies for stirring and heating respectively with values  
 270 of  $0.03 \text{ kWh}\cdot\text{kg}_{BioD}^{-1}\cdot\text{y}^{-1}$  and  $2.1 \text{ MJ}\cdot\text{kg}_{BioD}^{-1}\cdot\text{y}^{-1}$  respectively.

### 271 **2.2.8 Fermentation: R-401**

Another stirred reactor R-401 was considered to perform the fermentation reaction. It takes as input the mass of carbohydrates contained in the S-205 stream,  $M_{Sg,205}$ . The simulation used the values reported by Karemore and Sen [56], which also deal with lipid extraction followed by chemical pretreatment of the residual biomass with  $\text{H}_2\text{SO}_4$  (not simulated) and fermentation

by *Saccharomyces cerevisiae*. Under this protocol 90% of carbohydrates  $\eta_{Fer,Sg}$ , were converted into bioethanol with a yield  $Y_{Fer}$ ,  $0.23 \text{ kg}_{BioE} \cdot \text{kg}_{Sg}^{-1}$  (theoretical yield of Ethanol conversion,  $0.51 \text{ kg}_{BioE} \cdot \text{kg}_{Sg}^{-1}$  [73, 74]). Calculations used to describe the fermentation process were:

$$M_{BioE,402} = M_{Sg,205} \cdot Y_{Fer} \quad (49)$$

$$M_{Sg,402} = M_{Sg,205} \cdot (1 - \eta_{Fer,Sg}) \quad (50)$$

The energy consumption was based on the specific power  $P_{El,R401}$  related to the algal biomass produced in PBR-101, accounting  $0.05 \text{ MJ} \cdot \text{kg}_{DW}^{-1}$ :

$$E_{Input,R401} = P_{El,R401} \cdot M_{X,102} \cdot t_{OP} \quad (51)$$

## 2.2.9 Bioethanol and Biodiesel purification unit: D-402 and D-303

The final stages in bioethanol and biodiesel production are the purification units D-402 and D-302 respectively. The same set of equations were used for both processes. It was considered the operation efficiency (90% for  $\eta_{D402}$  and  $\eta_{D303}$ ) and final purity of the corresponding biofuel (95% for  $Pu_{D402}$  and  $Pu_{D303}$ ). The final liquid biofuel is recovered in the streams S-403 ( $M_{BioE,403}$ ,  $\text{kg} \cdot \text{d}^{-1}$ ) for bioethanol, and S-305 for biodiesel ( $M_{BioD,305}$ ,  $\text{kg} \cdot \text{d}^{-1}$ ). This leads to the following equations:

$$M_{BioD,305} = M_{BioD,304} \cdot \eta_{D303} \cdot Pu_{D303} \quad (52)$$

$$M_{TAG,305} = M_{TAG,304} \cdot \eta_{D303} \cdot (1 - Pu_{D303}) \quad (53)$$

$$M_{BioE,403} = M_{BioE,402} \cdot \eta_{D402} \cdot Pu_{D402} \quad (54)$$

$$M_{Sg,403} = M_{Sg,402} \cdot \eta_{D402} \cdot (1 - Pu_{D402}) \quad (55)$$

No particular technology for the purification of both biofuels was suggested in calculations, therefore energy consumption was not considered. Note that some purification processes for

275 bioethanol, like distillation, which could be high energy-consuming, were not included here. This  
 276 aspect will be discussed later.

### 277 2.3 Output calculations

278 Three different energy outputs were obtained from simulations: the theoretical energy content of  
 279 the biomass  $E_X$ , the potentially recoverable fuel energy  $E_P$ , and the actual total energy  $E_T$ .

The theoretical energy content of the biomass  $E_X$  considered a heating value for algae biomass  $H_{AlgX}$  of  $25.7 \text{ MJ}\cdot\text{kg}_{DW}^{-1}$  reported by Tibbetts et al. [75], and it was computed as follows:

$$E_X = M_{X,103} \cdot H_{AlgX} \cdot t_{OP} \quad (56)$$

280 As biomass production for all the simulation cases was set at  $1 \text{ t}\cdot\text{y}^{-1}$ , the theoretical energy content  
 281 is  $25\,700 \text{ MJ}\cdot\text{t}^{-1}\cdot\text{y}^{-1}$  also for all scenarios.

The potentially recoverable total fuel energy  $E_P$  was described by Heredia et al. [19] as the energy that can be recovered in a 100% efficient process, and so it shows the maximum energy achievable from biomass energy-rich compounds (TAG and carbohydrates). Here is presented per each Ton of biomass produced ( $\text{MJ}\cdot\text{t}^{-1}\cdot\text{y}^{-1}$ ). It sums the potentially recoverable biodiesel energy  $E_{P,BioD}$  ( $\text{MJ}\cdot\text{t}^{-1}\cdot\text{y}^{-1}$ ) and the potentially recoverable bioethanol energy  $E_{P,BioE}$  ( $\text{MJ}\cdot\text{t}^{-1}\cdot\text{y}^{-1}$ ) for a double biofuel recovery. In addition, calculations of potentially recoverable biodiesel and bioethanol energies considered the maximum theoretical yield in the stoichiometric reactions, which leads to:

$$E_{P,BioD} = (S_X \cdot \%_X TAG / MW_{AlgLip}) \cdot \eta_{E,TAG} \cdot 3 \cdot Y_{Trans} \cdot MW_{FAME} \cdot \Delta H_{comb,BioD}^\circ \cdot A^* \cdot t_{OP} \quad (57)$$

$$E_{P,BioE} = (S_X \cdot \%_X Sg) \cdot \eta_{E,Sg} \cdot Y_{Fer} \cdot \Delta H_{comb,BioE}^\circ \cdot A^* \cdot t_{OP} \quad (58)$$

$$E_P = E_{P,BioD} + E_{P,BioE} \quad (59)$$

282 As it can be noted in the calculation of the potentially recoverable total fuel energy  $E_P$ , it was  
 283 considered a 100% extraction recovery efficiency for TAG and carbohydrates ( $\eta_{E,TAG}$  and  $\eta_{E,Sg}$ ).  
 284 The same was considered for the transesterification yield  $Y_{Trans}$ , but not for the fermentation yield  
 285  $Y_{Fer}$ , where Lee et al. [73], Okamoto et al. [74] have referred a  $0.51 \text{ kg}_{BioE}\cdot\text{kg}_{Sg}^{-1}$  for the theoretical

286 value. The heat of combustion of biodiesel and bioethanol  $\Delta H_{comb}^{\circ}$  were 40.4 and 26.7 MJ·kg $_{BioFuel}^{-1}$   
 287 respectively [29, 76, 77]. Note that the illuminated surface  $A^*$  in Eq. 57 and 58 for the culture  
 288 system is specific for each simulation case.

Likewise, the actual energy obtained from biodiesel  $E_{BioD}$  and bioethanol  $E_{BioE}$  per 1 t of biomass here simulated (MJ·t $^{-1}$ ·y $^{-1}$ ) were calculated as follows:

$$E_{BioD} = M_{BioD,305} \cdot \Delta H_{comb,BioD}^{\circ} \cdot t_{OP} \quad (60)$$

$$E_{BioE} = M_{BioE,403} \cdot \Delta H_{comb,BioE}^{\circ} \cdot t_{OP} \quad (61)$$

Some simulations also included the co-production of photovoltaic energy  $E_{PV}$  (MJ·t $^{-1}$ ·y $^{-1}$ ) in the PBR-101. This was calculated based on the values reported by Nwoba et al. [28], where each installed PBR of 1.8m $^2$  produced 110.2 kWh·y $^{-1}$  (for a solar irradiance from 16 to 28 MJ·m $^{-2}$ ·y $^{-1}$  and from 7 to 9 sunlight hours per day). This brings a PV areal power  $P_{PV,PBR101}$  of 61.23 kWh·m $^{-2}$ ·y $^{-1}$ . The PV energy recovered at the culture unit may be then calculated as follows:

$$E_{PV} = P_{PV,PBR101} \cdot A^* \quad (62)$$

Therefore, the actual total energy produced by the simulated process is the sum of the latter equations including, if mentioned, the PV energy produced in PBR-101. The final energy output of a simulated process is then:

$$E_T = E_{BioD} + E_{BioE} + E_{PV} \quad (63)$$

Finally, the net energy ratio  $NER$  was calculated as follows:

$$NER = E_{output}/E_{input} \quad (64)$$

289 where  $E_{input}$  accounts for the sum of all the energy inputs for each equipment previously described in  
 290 the corresponding simulation case. Note that  $E_{output}$  can be replaced with any other energy output  
 291 previously described (or with any other partial energy) to represent different  $NER$  assumptions.  
 292 Such values may differ from each other even though simulation cases were conducted for the same

293 yearly produced biomass ( $1 \text{ t}\cdot\text{y}^{-1}$ ).  $NER$  values were retrieved in this study as:

294 a) using the maximum energy content:

- 295 •  $NER_X$ : considering the theoretical energy content of the biomass  $E_X$ ,
- 296 •  $NER_{EP}$ ,  $NER_{EP,BioD}$  or  $NER_{EP,BioE}$ : considering the potentially recoverable total
- 297 fuel energy  $E_P$ , or the corresponding partial values  $E_{P,BioD}$  or  $E_{P,BioE}$ ,

298 b) using the actual energy for the simulation case (including or not the photovoltaic energy

299  $E_{PV}$ ):

- 300 •  $NER_T$ ,  $NER_{EBioD}$  or  $NER_{EBioE}$  considering the actual total energies  $E_T$ , or the actual
- 301 partial energies  $E_{BioD}$  or  $E_{BioE}$  for a simulation case.

302 Therefore an energy-positive process will have values greater than or equal to 1.

## 303 2.4 Simulation Cases Description

304 Eight simulation cases have been proposed in this work to simulate  $1 \text{ t}\cdot\text{y}^{-1}$  of microalgae culture.

305 Relevant and cumulative changes in operation blocks are added to complete and follow the also

306 cumulative  $NER_T$  improvement from case to case.

307 In contrast to operation blocks Prod-100 and Rec-200, technologies for operation blocks BioD-

308 300 and BioE-400 have been maintained for all the cases, except for the D-301 unit in case 6.

309 Some other minor considerations regarding the size or power of equipment may have been adapted

310 in each case to treat the resultant flow rate. Main process values in the culture unit (*eg.* PBR

311 technology description, strains, and culture productivities) are summarized in Table 1. Other minor

312 descriptions and those related to downstream treatment are detailed below:

313 **Case 1:** The first simulation considers the dry-pathway for biodiesel production only and an

314 ideal strain. The PBR-101 unit is a raceway pond of 15 cm in depth. No thermal

315 regulation technology has been considered as it will be discussed in Section 3.1. The

316 culture was supposed in continuous mode with an ideal strain based on Pruvost et al.

317 [24]. The downstream operations here considered were: i) concentration unit using

318 centrifugation as the C-102 unit, and collecting biomass at  $\%_{W,C102}$  of 80% w/w (*ie.*

319  $200 \text{ kg}\cdot\text{m}^{-3}$ ); ii) pretreatment unit with a thermal dryer TD-201 and  $\%_{DW,TD102}$  of

320 100% (fully dry); iii) for the lipid recovery unit, a centrifugal L-L extractor using  
321 n-hexane as solvent; and iv) all the BioD-300 block;

322 **Case 2:** This simulation uses the wet-pathway for biodiesel production only and an ideal strain.  
323 The PBR-101 unit is also a raceway pond of 15 cm depth following the same consid-  
324 eration for no thermal regulation technology. Culture mode and strain were the same  
325 as in case 1. The downstream operations considered here were: i) harvesting biomass  
326 using flotation as the Fl-102 unit, and concentrating at  $\%_{W,Fl102}$  of 99% w/w (*ie.* 10  
327  $\text{kg}\cdot\text{m}^{-3}$ ), ii) pretreatment unit with a bead miller BM-201 achieving 80% of disruption  
328 rate, iii) for the lipid recovery, an S-L extractor using 2-methyl-tetra-hydrofuran as a  
329 solvent, and iv) the entire BioD-300 block.

330 **Case 2.a.** was proposed as a variation of Case 2, for adding the block BioE-400 for  
331 bioethanol production (*ie.* double biofuel recovery)

332 **Case 3:** Simulation considers also the wet-pathway for double biofuel recovery and an ideal  
333 strain. In this case, the PBR-101 includes the intensified culture technology of high  
334 volumetric productivity photobioreactor HVP, also referred to as AlgoFilm<sup>©</sup> [26, 27].  
335 The culture unit PBR-101 is 2 mm in depth. In addition, the operation unit included  
336 the use of an insulated-glazed unit IGU [28] with which the need for thermal regulation  
337 is no longer required. Culture production mode and strain were the same as in pre-  
338 vious cases. For downstream operations: i) no concentration unit was required since  
339 HVP PBR biomass concentration was high enough for the ii) bead miller BM-201,  
340 which was considered again for an 80% of disruption rate; iii) then an S-L extractor  
341 was proposed using 2-methyl-tetra-hydrofuran as a solvent; iv) the BioD-300 block;  
342 and v) the BioE-400 block was included again.

343 **Case 3.a.** completes Case 3 with a PV panel at the PBR-101 unit as described  
344 in Nwoba et al. [28], which enables to produce PV energy in addition to the double  
345 biofuel recovery.

346 **Case 4:** Simulation is for the wet-pathway for double biofuel recovery and PV energy co-  
347 production, and an actual strain. It takes into account the same upstream and down-

348 stream operations as in case 3.a., but now considering experimental values reported  
349 for the nitrogen-limited culture of *Nannochloropsis gaditana* according to Heredia  
350 et al. [19]. The values used for the simulation are presented in Table 1.

351 **Case 5:** The wet-pathway for the double biofuel recovery with PV energy co-production is  
352 maintained for this scenario with an ideal strain. The culture in an HVP+IGU  
353 photobioreactor has been considered once more but with a variable output biomass  
354 concentration for testing the interest of such an increase in the downstream processing.  
355 Operations units for the downstream processing were i) a band filtration F-102 unit  
356 enabling to concentrate of the biomass to an optimum value (further discussed); ii) a  
357 bead miller BM-201 as shown for in the previous cases; iii) an S-L extractor using  
358 2-methyl-tetra-hydrofuran as a solvent, which was supposed to work at the same  
359 optimum F-102 value and, as consequence avoid the S-202 dilution stream; iv) and  
360 finally the BioD-300 and v) the BioE-400 blocks.

361 **Case 6:** For the last scenario, also the wet-pathway for double biofuel recovery with PV energy  
362 co-production from an ideal strain was proposed. The production process was the  
363 same as in Case 5 except for the lipid recovery unit where a decantation operation  
364 Dec-202 was proposed to simulate the avoidance of a solvent-based process. The  
365 followed operation blocks remained the same.

## 366 3 Results and Discussion

### 367 3.1 Culture system impact on energy balance

368 The cultivation step alone can induce a significant energy expenditure. This energy expenditure is  
369 mainly due to two items, namely thermal regulation and mixing.

370 The energy consumption of a microalgae culture system is highly dependent on the technology  
371 used [60, 28, 78, 79]. For example, closed photobioreactor technologies are known to be subjected  
372 to overheating, which is more limited in open systems because of water evaporation. It is also very  
373 much related to the targeted range of temperature and level of control applied. It was investigated  
374 in detail in Pruvost et al. [80] for open raceway used in harsh desert conditions. A temperature

375 regulation of 35 °C (*ie.* optimal temperature of a thermal resistant strain) during the summer period  
376 led to the energy consumption of 16.7 kWh·m<sup>-2</sup>·d<sup>-1</sup>, whereas leaving the possibility of temperature  
377 drift in the range of 28 - 40 °C led to 3.8 kWh·m<sup>-2</sup>·d<sup>-1</sup>. This may be applied to a closed system, but  
378 ultimately with higher energy consumption, due to the absence of evaporation to naturally reduce  
379 heating. Pruvost et al. [81] estimated the yearly energy consumption linked to thermal regulation  
380 of vertical PBR at around 500 - 1000 kWh·m<sup>-2</sup> for France location (*ie.* 1.4 - 2.8 kWh·m<sup>-2</sup>·d<sup>-1</sup>)  
381 but peak values are encountered in summer and winter periods. For example Pérez-López et al.  
382 [78] presented a detailed study with data for different periods other the year, emphasizing a 15 and  
383 5-fold increase between summer and winter, and between summer and fall respectively. Although  
384 energy requirements highly depend on several conditions (*ie.* technology, location, period of the  
385 year, targeted temperature range), it can be emphasized that thermal regulation alone may lead  
386 to very large energy needs.

387 The same conclusion may be made with the energy requested for mixing. In general, mixing  
388 energy is related to culture volume [82, 83]. Airlift technologies as well as tubular PBRs are  
389 also known to have high energy consumption due to significant pressure drops, with electrical  
390 power consumption in the range 300 – 2000 W·m<sup>-3</sup>. For example, Norsker et al. [84] reported  
391 an electrical power value for mixing of 30 W·m<sup>-2</sup> for an airlift system of 2cm depth, leading to  
392 1500 W·m<sup>-3</sup>. Conversely, raceway-type cultivation systems exhibit low to moderate consumption  
393 due to paddlewheel agitation and moderate pressure drops. Values are also highly dependent on  
394 the raceway design, culture depth, and paddle wheel rotation speed and design. Electrical power  
395 requirements in the range of around 0.25 - 4 W·m<sup>-2</sup> are usually reported (*ie.* 2 - 40 W·m<sup>-3</sup>)  
396 [60, 85, 86, 78, 59]. Note here the large difference when values are expressed per unit of culture  
397 volume between PBR (300 – 2000 W·m<sup>-3</sup>) and raceway (2 - 40 W·m<sup>-3</sup>). This is related to the  
398 large variation of culture volume per area of culture when comparing airlift PBR to raceway culture  
399 system (around a few liters to a few hundred liters per m<sup>2</sup> respectively) [87, 26]. Consequently,  
400 decreasing the culture volume (*ie.* depth of culture) will decrease the resulting energy needed for  
401 mixing. This will be investigated in this work.

402 Both energies for mixing and thermal regulation show the wide range of energy consumption on  
403 the cultivation stage. Thermal regulation in the range of 1 - 4 kWh·m<sup>-2</sup>·d<sup>-1</sup> are usually encountered  
404 (possibly with significant higher values depending on the climate-species-culture system adequacy).

405 For a 12 h mixing per day (*ie.* no mixing during the night), energy for mixing will range between  
406 0.024 - 0.48 kWh·m<sup>-3</sup>·d<sup>-1</sup> and 3.6 - 24 kWh·m<sup>-3</sup>·d<sup>-1</sup> for raceway and airlift PBR respectively,  
407 corresponding approximately to 2.4 - 48 Wh·m<sup>-2</sup>·d<sup>-1</sup> for a raceway of 10 cm depth, and to 72 -  
408 480 Wh·m<sup>-2</sup>·d<sup>-1</sup> for an airlift PBR of 2 cm depth.

409 Considering a biomass calorific value of about 20 MJ·kg<sup>-1</sup> (*ie.* 5.56 kWh·kg<sup>-1</sup>) and a maximum  
410 biomass productivity of 11 - 27 g·m<sup>-2</sup>·d<sup>-1</sup> (40 - 100 t·ha<sup>-1</sup>·y<sup>-1</sup>), energy recoverable from microalgal  
411 biomass can be estimated in the range 0.06 - 0.15 kWh·m<sup>-2</sup>·d<sup>-1</sup> [81]. Increasing the energy-  
412 rich biomolecules in the cell by applying for example a growth limitation by nitrogen source will  
413 increase such a value. In this regard, Illman et al. [88] reported a calorific value of 21 MJ·kg<sup>-1</sup>  
414 and 29 MJ·kg<sup>-1</sup> with *Chlorella emersonii* with 29% and 63% in total lipids respectively. But such  
415 limitation will be also detrimental to biomass productivity (as shown later). A maximal value of  
416 recoverable energy in the biomass of 0.15 kWh·m<sup>-2</sup>·d<sup>-1</sup> (540 kJ·m<sup>-2</sup>·d<sup>-1</sup>) can then be considered  
417 as a good upper limit in first instance (as described later, Heredia et al. [19] estimated a potentially  
418 recoverable biofuel energy at 19 642 MJ·t<sup>-1</sup>·y<sup>-1</sup>, corresponding to 0.003 - 0.002 Wh·m<sup>-2</sup>·d<sup>-1</sup>).  
419 This shows that it is easy to have a much higher energy consumption in the culture stage than that  
420 recoverable in biomass, even without introducing energy needs for downstream processing of the  
421 biomass up to biofuel conversions.

422 To simplify the analysis presented here, only two main categories of technologies were retained  
423 for simulations, both assuming that thermal regulation was negligible leading to little energy con-  
424 sumption: a raceway culture system without thermal regulation, and a closed PBR with passive  
425 thermal regulation. In both cases, the temperature was assumed to be maintained in the range of  
426 optimal growth all over the year. Passive thermal regulation for closed PBRs could be found as an  
427 optimistic hypothesis, but such a principle was introduced recently by Nwoba et al. [28] using an  
428 insulated-glazed photovoltaic photobioreactor and also discussed in Goetz et al. [89] where phase  
429 change materials and IR filtering were combined for passive regulation. As a result, energy con-  
430 sumed at the culture stage was then only related to mixing. It was fixed at 0.368 kWh·m<sup>-3</sup>·d<sup>-1</sup>  
431 hereafter (data obtained in our facility from experiments on raceways systems of various depths, in  
432 accordance with literature).

Table 2: Input/output energies and liquid biofuel volumes produced for the simulated cases. All the values correspond to a total production of  $1 \text{ t}\cdot\text{y}^{-1}$  of microalgal biomass.

Case		1	2 & 2.a.	3 & 3.a.	4	5	6						
		<i>a) Input Energies, <math>E_{input} \text{ (MJ}\cdot\text{t}^{-1}\cdot\text{y}^{-1}\text{)}</math></i>											
Prod-100	PBR-101	238 714	12 067	12 067	12 067	437	437	485	485	626	437	626	437
	102	226 647	12 067	595	437	0	485	0	626	189	626	189	189
Rec-200	201	15 293	9 027	4 370	4 370	4 370	4 370	5 159	4 370	5 159	4 370	4 370	4 370
	202	6 266	5 159	788	5 159	788	788	5 159	788	5 159	788	4 370	0.1
BioD-300	D-301	5 430	4 745	67 511	67 000	67 511	67 000	67 210	67 000	4 163	3 652	578	0
	R-302	684	511	511	511	511	210	210	511	511	578	578	578
BioE-400	R-401	-	-	50	50	50	50	50	50	50	50	50	50
		259 436	85 381	73 157	72 903	9 998	5 625						
		<i>b) Biofuel Produced volume (<math>\text{L}\cdot\text{t}^{-1}\cdot\text{y}^{-1}\text{)}</math></i>											
BioD		311	232	232	95	232	262						
BioE			95	95	55	95	95						
Total BioFuel		311	327	327	150	327	357						
		<i>c) Output Energy (<math>\text{MJ}\cdot\text{t}^{-1}\cdot\text{y}^{-1}\text{)}</math></i>											
$E_{BioD}$		10 705	7 993	7 993	3 286	7 993	9 040						
$E_{BioE}$			2 004	2 004	1 152	2 004	2 004						
$E_{PV}$				36 689	40 666	36 689	36 689						
$E_T$		10 705	9 997	46 686	45 105	46 686	47 732						

Table 3: Net Energy Ratio from the different energy sources at each simulation case. All the values correspond to a total production of  $1 \text{ t}\cdot\text{y}^{-1}$  of microalgal biomass.

Case		1	2 & 2.a.	3 & 3.a.	4	5	6
		<i>a) Maximum energy content</i>					
	$NER_X$	0.099	0.301	0.351	0.353	2.571	4.569
	$NER_{EP,BioD}$	0.055	0.166	0.194	0.080	1.420	2.524
	$NER_{EP,BioE}$	0.021	0.064	0.074	0.043	0.545	0.968
	$NER_{EP}$	0.076	0.230	0.268	0.123	1.965	3.492
		<i>b) Simulated recovered energy</i>					
- $E_{PV}$	$NER_{EBioD}$	0.04	0.09	0.11	0.05	0.80	1.61
	$NER_{EBioE}$		0.02	0.03	0.02	0.20	0.36
	$NER_T$	0.04	0.12	0.14	0.06	1.00	1.96
+ $E_{PV}$	$NER_{EBioD}$			0.61	0.60	4.47	8.13
	$NER_{EBioE}$			0.53	0.57	3.87	6.88
	$NER_T$			0.64	0.62	4.67	8.49

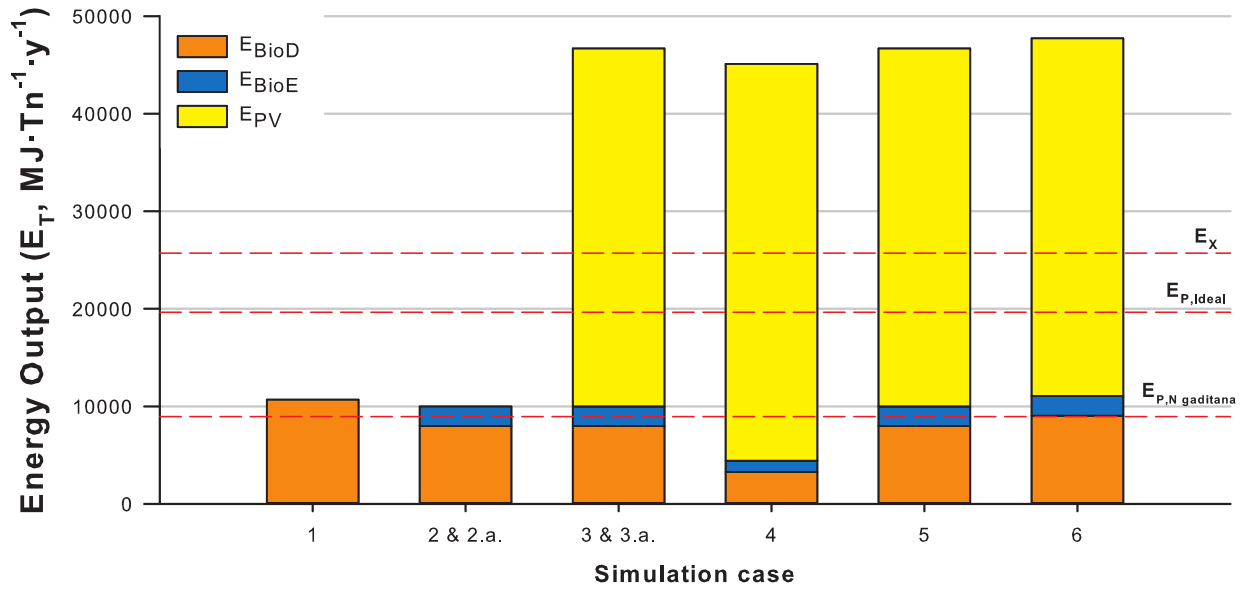
### 433 3.2 Cases comparisson

434 Table 1 includes the potentially recoverable energy values for each biofuel produced in each scenario.

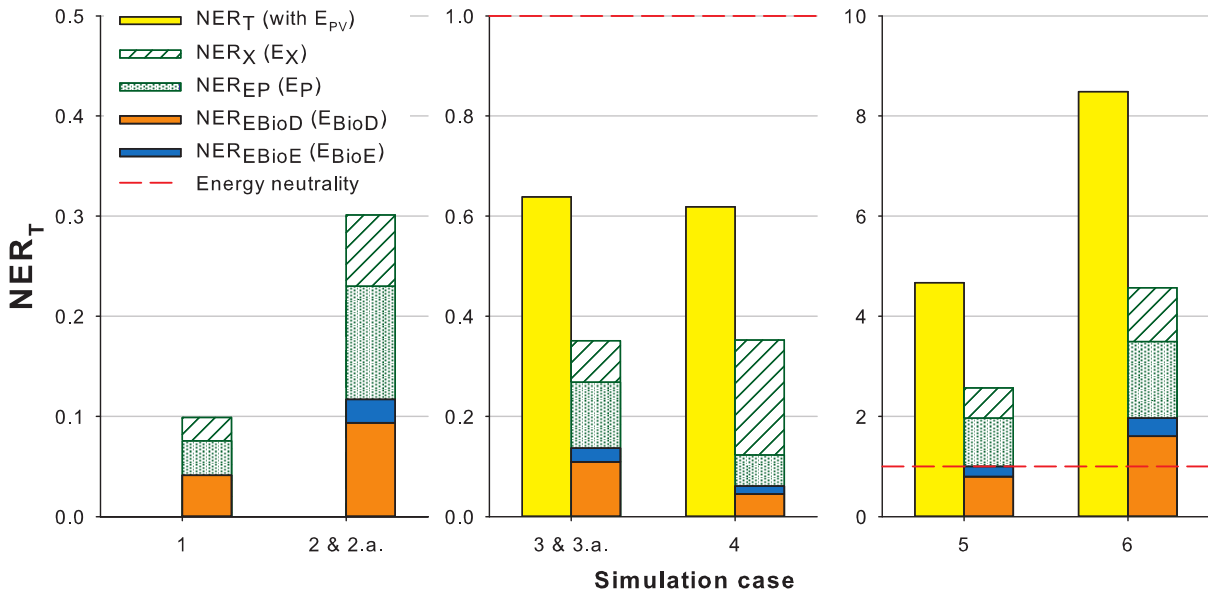
435 The corresponding actual input/outputs energy values are described in Table 2 and represented

436 in Figure 2a. The corresponding maximum and actual  $NER$  values are presented in Table 3 and

437 Figure 2b.



(a)



(b)

Figure 2: Energy output a) and  $NER_T$  b) comparison for the simulated cases. Red-dashed lines are: a) reference for theoretical energy content of the biomass  $E_X$ , potentially recoverable energy  $E_{P,Ideal}$  for the ideal strain, potentially recoverable total fuel energy  $E_{P,Ngaditana}$  for *N. gaditana*, and b) energy neutrality ( $NER_T = 1$ ).

438 **3.2.1 Cases 1 and 2 & 2.a.: Dry and Wet-pathway comparison, and Double biofuel**  
 439 **recovery**

440 Using an ideal strain, the biodiesel production process under a classical dry-pathway (Case 1) and  
 441 a wet-pathway (Case 2) resulted in  $NER_T$  equal to 0.04 and 0.09 respectively, which are much  
 442 below the energy neutrality. Both process may recover  $E_{P,BioD}$  up to 14 196  $\text{MJ}\cdot\text{t}^{-1}\cdot\text{y}^{-1}$ , however  
 443 in Case 1 it was only recovered 10 705  $\text{MJ}\cdot\text{t}^{-1}\cdot\text{y}^{-1}$  of  $E_{BioD}$  ( $311 \text{ L}\cdot\text{t}^{-1}\cdot\text{y}^{-1}$ ) and consumed  $E_{input}$   
 444 of 259 436  $\text{MJ}\cdot\text{t}^{-1}\cdot\text{y}^{-1}$ . In comparison, Case 2 produced 7 993  $\text{MJ}\cdot\text{t}^{-1}\cdot\text{y}^{-1}$  of  $E_{BioD}$  but consumed  
 445 only  $E_{input}$  of 85 381  $\text{MJ}\cdot\text{t}^{-1}\cdot\text{y}^{-1}$ . In other words, Case 1 recovered only around 34% more biodiesel  
 446 energy than Case 2 (2 712  $\text{MJ}\cdot\text{t}^{-1}\cdot\text{y}^{-1}$  more), but also Case 1 consumed 3 times more energy than  
 447 Case 2.

448 The dry-pathway consumed most of the energy, 238 714  $\text{MJ}\cdot\text{t}^{-1}\cdot\text{y}^{-1}$ , (*ie.* 92% of the  $E_{input}$ )  
 449 during the Prod-100 block. The raceway culture system produced  $0.13 \text{ kg}\cdot\text{m}^{-3}$  of biomass in 166  
 450  $\text{m}^2$ , which was concentrated to  $200 \text{ kg}\cdot\text{m}^{-3}$  (80%<sub>W,C102</sub>, w/w), which is the recommended value  
 451 prior to the thermal dryer TD-201 unit [63]. Then the recovery block R-200 consumed 15 293  
 452  $\text{MJ}\cdot\text{t}^{-1}\cdot\text{y}^{-1}$  (6% of the  $E_{input}$ ) including 9 027  $\text{MJ}\cdot\text{t}^{-1}\cdot\text{y}^{-1}$  for the thermal dryer TD-201 only.

453 Besides, the wet-pathway consumed most of the energy at the BioD-300 block, representing 79%  
 454 of the corresponding  $E_{input}$  with 67 511  $\text{MJ}\cdot\text{t}^{-1}\cdot\text{y}^{-1}$ . Almost the entire of this energy consumption  
 455 (99%) was due to the need for evaporating  $178 \text{ t}\cdot\text{y}^{-1}$  of extraction solvent at D-301 unit. Such an  
 456 amount of solvent was a consequence of the low productivity associated with the raceway culture  
 457 system (in 15 cm depth) and the eventual dilution (from 10 to  $7.9 \text{ kg}\cdot\text{m}^{-3}$ ) for reaching an optimal  
 458 disrupted-biomass concentration for the L-L extraction (Heredia et al. [44]). The resulting 127  
 459  $\text{t}\cdot\text{y}^{-1}$  were then treated using the 1.65  $S/F$  ratio.

460 Biodiesel production via the wet-pathway is shown here to be a more energetically viable process  
 461 compared to the dry pathway. However, note as well that Case 1 also obtained a  $NER_{EBioD}$  of 75%  
 462 of the maximum recoverable  $NER_{EP,BioD}$  (42% of  $NER_X$ ), and Case 2 a  $NER_{EBioD}$  of 56% of the  
 463 corresponding maximum  $NER_{EP,BioD}$  (39% of  $NER_X$ ). This highlights a potential optimization in  
 464 the wet-pathway to not only develop intensified efficient technologies with low-energy consumption  
 465 but also processes that would allow treating high biomass concentrations ( $>10 \text{ kg}\cdot\text{m}^{-3}$ ) during the  
 466 lipid recovery step.

467 Increasing the energy output is another way to improve the  $NER_T$ . Simulation case 2.a.  
468 includes the additional recovery of bioethanol after valorization of the carbohydrates in the non-  
469 extracted residues of the centrifugal extractor. Such a process, as part of an energy-driven biore-  
470 finery approach, aimed to increase the energy output of the biofuel production process [56, 55, 57].

471 The  $NER_T$  considering such double biofuel recovery has only increased to 0.12, but recovering  
472 now  $327 \text{ L}\cdot\text{t}^{-1}\cdot\text{y}^{-1}$  of two liquid biofuels instead of the  $232 \text{ L}\cdot\text{t}^{-1}\cdot\text{y}^{-1}$  in a only-biodiesel wet-  
473 pathway process (representing 140% increase in volume of liquid biofuels). This indicates that  
474 the co-production of bioethanol does not improve the energy balance, but increases the amount  
475 of biofuel produced for given biomass. Notably, the double biofuel recovery takes advantage of  
476 the amount of carbohydrates and lipids available in the cell to be converted into liquid biofuels.  
477 Therefore, microalgae culture protocols where biomass accumulates large amounts of these energy-  
478 rich molecules, are ideal for this approach.

479 Even if the fermentation and recovery process are optimized at the maximum yields, the double  
480 biofuel recovery might remain below the energy neutrality ( $NER_{EP}$  of 0.23). Note from Tables 1  
481 and 2, that the actual recovered energy differs in about 65% of the  $E_{P,BioE}$ . Bear in mind that the  
482 final yield for the microalgal biomass hydrolysis and the subsequent fermentation is significantly  
483 lower than the theoretical value, even for separated processes [90, 91]. Klinke et al. [92] suggested  
484 that microalgae hydrolysate may contain inhibitory chemicals for ethanol fermentation which may  
485 reduce the yield. [91] suggested another process application known as the simultaneous sacchari-  
486 fication and fermentation (SSF) using carbohydrate-rich biomass and bacteria, which has yielded  
487 87.1% of the theoretical value (0.209 g ethanol/g biomass). Such a process is expected to be less  
488 inhibitory but it may take a longer operation time.

489 Note that energies for both biodiesel and bioethanol purification units (D-303 and D-402) were  
490 not considered here and might be different for both. Recovering the bioethanol from the fer-  
491 mentation broth or FAME's (biodiesel) from methanol traditionally requires a distillation process  
492 which may be more energy-consuming. For example, lower carbohydrate concentrations affect the  
493 bioethanol concentrations at the end of fermentation, hence more energy would be invested via a  
494 distillation process turning into a not energy-efficient the whole operation. Membrane technologies  
495 like those presented by Wei et al. [93] and Lewandowicz et al. [94] may be suitable for a more  
496 energy-efficient biofuel process.

497 The double biofuel recovery approach opens the way to the energy recovery from other sources in  
498 an energy-biorefinery perspective (*eg.* biohydrogen, methanization or PV energy) [95, 96, 1, 97, 28].

### 499 **3.2.2 Cases 3 & 3.a. and 4: Improvements for the Upstream processing**

500 By using the HVP+IGU photobioreactor with an ideal strain and integrating the double biofuel  
501 production during Case 3, the  $NER_T$  slightly increased to 0.14. For the same amount of energy  
502 and volume of liquid biofuels produced as in Cases 2 & 2.a., the energy input  $E_{input}$  was reduced in  
503 73 157 MJ·t<sup>-1</sup>·y<sup>-1</sup>. This represents a reduction of 14% in energy consumption due to the Prod-100  
504 block which only consumed 437 MJ·t<sup>-1</sup>·y<sup>-1</sup>.

505 The use of the HVP+IGU technology as a PBR-101 unit, not only removes the energy con-  
506 sumption due to thermal control but also discards the need for biomass concentration. Pruvost  
507 et al. [26] already discussed the PBR depth and light absorption optimization leading to higher  
508 biomass concentrations. By reducing the PBR depth to 2 mm, the biomass concentration reached  
509 9.53 kg·m<sup>-3</sup> and the final volume of the culture passed from 25 m<sup>3</sup> (for raceway PBR) to 0.33 m<sup>3</sup>  
510 (for HVP PBR) on the same surface. However such volume reduction was not enough to impact  
511 the amount of solvent used and the associated energy consumption for the evaporation, because  
512 the optimum biomass concentration for the CX-202 unit still requires a previous dilution to reach  
513 7.9 kg·m<sup>-3</sup>. The BioD-300 block still consumed 67 511 MJ·t<sup>-1</sup>·y<sup>-1</sup>.

514 Another relevant feature of HVP-PBR is the decrease in volume (*ie.* process intensification).  
515 Figure 3 compares the effect of the depth of the culture for raceway (Case 2) and HVP+IGU  
516 (Case 3) PBR on the final  $NER_{BioD}$  (Biodiesel only) and the  $NER_T$  (double biofuel recovery).  
517 Simulations indicated that the maximum  $NER_T$  of 0.14 is attained at depths less than 1 - 3 cm  
518 for raceway and, inferior to around 0.5 cm for HVP+IGU. Greater depths also induce losses in  
519  $NER$ , which are more pronounced for HVP+IGU, down to approximately 0.02, and to 0.08 for  
520 the raceway. This is explained by the mixing energy here considered, which was greater per unit  
521 volume for the HPV-PBR than for the raceway culture system. A raceway with a depth below  
522 a few centimeters would certainly be impossible to operate in practice, but Figure 3 emphasizes  
523 here the relevance of the mixing energy. By designing HVP-PBR with low mixing energy (as with  
524 AlgoFilm<sup>©</sup> PBR in Pruvost et al. [26]), a further gain in  $NER$  can be obtained. Whatever the  
525 mixing energy, Figure 3 demonstrates the interest of increasing specific illuminated surfaces on

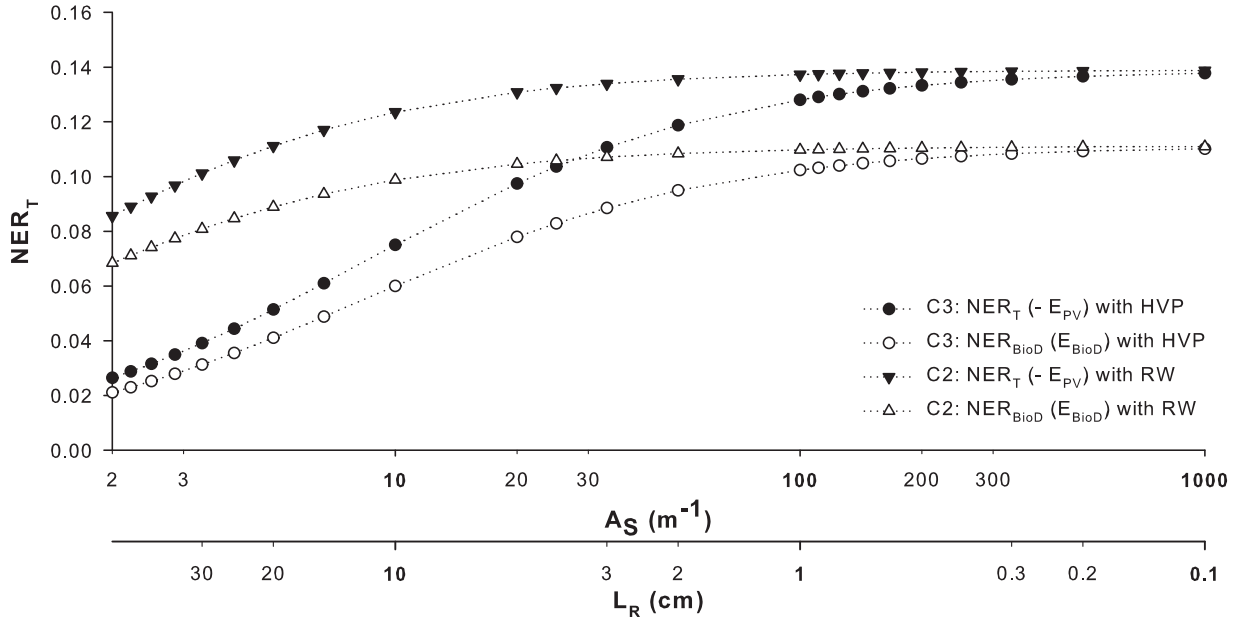


Figure 3: Impact of the depth of the culture using a raceway (Case 2) and a HVP+IGU (Case 3) photobioreactor on the  $NER_{BioD}$  and the  $NER_T$  during the wet-pathway biofuel production. The  $NER_T$  includes the double biofuel recovery but not the PV energy co-production.

526 the energy-saving for given biomass production. HVP+IGU PBR has for example values of the  
 527 specific illuminated surface around 75 higher than for raceway ( $500 m^{-1}$  to  $6.67 m^{-1}$ , Table 1),  
 528 then saving a significant amount of energy because of the culture volume reduction ( $0.3 m^3$  and 25  
 529  $m^3$  respectively).

530 In addition to the previous process, Case 3.a. adds the co-production of PV energy on the same  
 531 microalgae culture surface as suggested by Nwoba et al. [28]. PV panels coupled to HVP+IGU  
 532 PBR increased the  $NER_T$  to 0.64 which is 239% greater than the  $NER_{EP}$  and 182% more than the  
 533  $NER_X$ . The additional  $E_{PV}$  of  $36\,698 MJ \cdot t^{-1} \cdot y^{-1}$  is 50% of the  $E_{input}$  for the entire process. It can  
 534 be noted that this approach produced enough energy to sustain the entire Prod-100, Rec-200, and  
 535 BioE-400 blocks, and still contribute  $31\,043 MJ \cdot t^{-1} \cdot y^{-1}$  more for the BioD-300 block consumption.

536 Case 4 calculates the  $NER$  using experimental data obtained on *Nannochloropsis gaditana* (the  
 537 actual strain) and the process used in Cases 3 & 3.a.  $NER_T$  (without considering PV energy,  $-E_{PV}$ )  
 538 was reduced to 0.06, which is about half of the obtained with an ideal strain. The difference did not  
 539 only strive in the energy consumption of the process, which slightly decreased to  $72\,903 MJ \cdot t^{-1} \cdot y^{-1}$ ;  
 540 but in the energy obtained from biofuels, which was reduced in 44% to attain  $4\,438 MJ \cdot t^{-1} \cdot y^{-1}$   
 541 (where  $3\,286 MJ \cdot t^{-1} \cdot y^{-1}$  were issued from biodiesel and  $1\,152 MJ \cdot t^{-1} \cdot y^{-1}$  from bioethanol). The  
 542 biofuel volumes produced were reduced to  $150 L \cdot t^{-1} \cdot y^{-1}$  (95 and  $55 L \cdot t^{-1} \cdot y^{-1}$  of biodiesel and

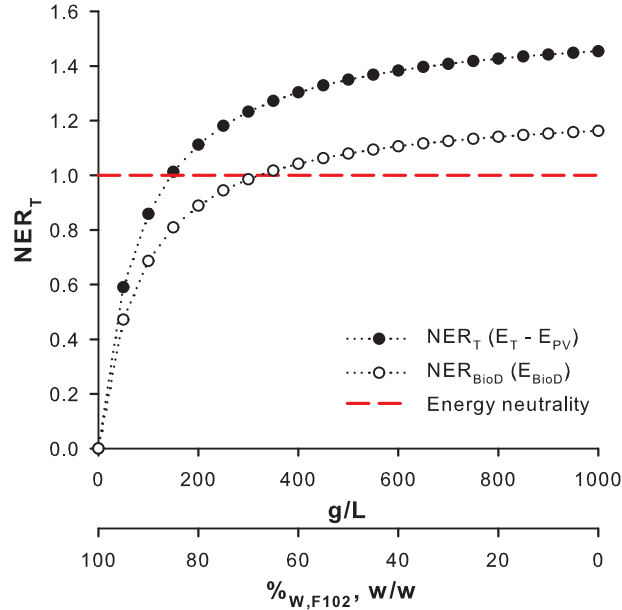


Figure 4: Impact of the harvesting biomass concentration (X-axis) on the  $NER_T$  using the band filtration F-102 unit. X-axis is also presented as moisture percentage ( $\%_{W,F102}$ , w/w). The black-circle plot consider the double biofuel recovery but not the PV energy; the white-circle plot is for a biodiese-only production process; and the values over the red dash line are considered as energy-neutral processes.

543 bioethanol respectively).

544 No significant changes were observed in energy consumption of production blocks  $E_{input}$ . The  
 545 losses in energy production were mainly only associated with the reduction in surface productivity  
 546 with *Nannochloropsis gaditana*. However, the losses may be compensated when co-producing PV  
 547 energy: with lower surface productivity, a larger culture surface of 185 m<sup>2</sup> was needed to produce  
 548 1 t·y<sup>-1</sup>, and thus more PV energy was available. This additional 40 666 MJ·t<sup>-1</sup>·y<sup>-1</sup> turned the  
 549  $NER_T$  to 0.62, a value similar to the obtained with an ideal strain in Cases 3 & 3.a.

550 The previous simulations, highlight the relevance of sharing the same illuminated surface be-  
 551 tween HVP+IGU PBR and PV panels, which may be a step forward in making energetically self-  
 552 sustaining the production of algae biofuels even when using savage strains. Nevertheless, the entire  
 553 process still needs optimization, mainly in key production blocks such as Rec-200 and BioD-300.  
 554 Other technology set-ups will be discussed below that may take better advantage of the previous  
 555 culture optimization for targeting better  $NER_T$  values.

### 556 3.2.3 Cases 5 & 6: Improvements for the Downstream processing

557 As discussed in section 3.2.2, the L-L extraction in CX-202 may play a major role in the *NER*  
558 because the lipid recovery is limited by the concentration of the disrupted cell suspension [44], and  
559 consequently, the resulting treated volume also impacts the energy consumption during solvent  
560 evaporation. The following Case 5 aims to elucidate the question of the optimal harvested biomass  
561 concentration to process maximal biomass with a minimum solvent in CX-202.

562 Using Case 3 as reference, the Figure 4 show the  $NER_T$  for 20 simulations issued of varying  
563 the harvested biomass concentration at F-102 unit. For retrieving  $NER_T$  values greater to energy  
564 neutrality ( $NER_T \geq 1$ ), concentration should be above to  $145 \text{ kg}\cdot\text{m}^{-3}$  ( $85.5\%_{W,F102}$ , w/w) con-  
565 sidering a double biofuel recovery (without including PV energy,  $-E_{PV}$ ); and above  $321 \text{ kg}\cdot\text{m}^{-3}$   
566 ( $68\%_{W,F102}$ , w/w) for a biodiese-only production process.

567 These values imply as well that operation units BM-201 and CX-202 should operate in the  
568 same concentration intervals as F-102. Bead milling may treat concentrations in the 1 to  $145$   
569  $\text{kg}\cdot\text{m}^{-3}$  range, with direct impact on the cell disruption rate and energy consumption [98, 99, 35–  
570 37]. However, the treatment at such high biomass concentration in centrifugal extractions may  
571 be limited by the emulsion formation, and the solvent-to-feed or partition ratios. Only the range  
572 2 to  $10 \text{ kg}\cdot\text{m}^{-3}$  has been investigated to date [100, 44, 43] and it should then request further  
573 investigation.

574 Band filtration, as F-102 unit, is a reliable option to achieve concentrations up to 200-300  
575  $\text{kg}\cdot\text{m}^{-3}$  [63]. It may be argued that flocculation, as a low energy consumption technology is ideal  
576 for this concentration step [101, 5]. However, adding either organic (*eg.* chitosan or guar gum which  
577 is carbohydrate-based) or inorganic (like  $FeCl_3$  or  $Al_2SO_4$ ) agents may fake yields or interfere with  
578 future chemical reactions as fermentation or transesterification. More important, flocculation does  
579 not concentrate enough of the biomass within the treatment limits of the next operations units  
580 [102–104]

581 It is also important to highlight that high biomass concentration processes may also reduce the  
582 water consumption in the system. This has not only an impact on the energy consumption but  
583 also the water footprint of microalgal biofuel production (which is already lesser than crop-based  
584 fuels as described by Pugazhendhi et al. [105]).

585 For a process at  $NER_T = 1$  ( $-E_{PV}$ ) with harvested biomass of  $145 \text{ kg}\cdot\text{m}^{-3}$  by band filtration,  
586  $9\,998 \text{ MJ}\cdot\text{t}^{-1}\cdot\text{y}^{-1}$  were consumed in total. In Case 5 the Rec-200 and BioD-300 were blocks that  
587 consumed the most with 52% and 42% of the  $NER_T$  ( $-E_{PV}$ ) respectively, but with only 5 159  
588  $\text{MJ}\cdot\text{t}^{-1}\cdot\text{y}^{-1}$  and  $4\,163 \text{ MJ}\cdot\text{t}^{-1}\cdot\text{y}^{-1}$ ) respectively, which is much lower than for Case 3.a. Working at  
589 larger biomass concentrations results in a large reduction in energy consumption (18 times) at the  
590 D-301 unit by saving especially water, thus amount of solvent and so the energy for final solvent  
591 evaporation, obtaining  $NER_{EP}$  and  $NER_X$  values of around 1.96 and 2.6 respectively. Even  
592 though the PV energy is no longer necessary to achieve a positive energy balance for the process  
593 in Case 5, an additional  $36\,689 \text{ MJ}\cdot\text{t}^{-1}\cdot\text{y}^{-1}$  would be produced ( $46\,686 \text{ MJ}\cdot\text{t}^{-1}\cdot\text{y}^{-1}$  in total), for  
594 finally recovering 4.67 times more energy than the invested for the whole process ( $NER_T$  with  
595  $E_{PV}$ ).

596 As may be inferred from the above Case 5, the use of solvents in the wet-pathway biofuel  
597 production may have a strong impact on the net energy ratio of the process, therefore it is essen-  
598 tial to either increase the operational work concentration of the metabolite recovery block or use  
599 technologies that do not rely at all on solvents.

600 In this regard, Case 6 simulates a process at the same previous biomass concentration but  
601 substitutes now the centrifugal extraction with a decantation process (no solvents involved). Such  
602 process is energetically self-sustaining without a double biofuel recovery ( $NER_{EBioD}$  of 1.61) or  
603 PV co-production ( $NER_T - E_{PV}$  of 1.96) but, if included, the final  $NER_T$  may result in the value  
604 of 8.49. The resultant process produces  $357 \text{ L}\cdot\text{t}^{-1}\cdot\text{y}^{-1}$  or  $11\,044 \text{ MJ}\cdot\text{t}^{-1}\cdot\text{y}^{-1}$  from liquid biofuels  
605 only. Additional  $E_{PV}$  ( $36\,689 \text{ MJ}\cdot\text{t}^{-1}\cdot\text{y}^{-1}$ ) will increase the  $E_T$  to  $47\,732 \text{ MJ}\cdot\text{t}^{-1}\cdot\text{y}^{-1}$ , which is not  
606 much different from the final energy production from Case 5. However, the use of a decantation  
607 Dec-202 unit reduced the energy consumption at the Rec-200 block to only  $4\,370 \text{ MJ}\cdot\text{t}^{-1}\cdot\text{y}^{-1}$ .  
608 As consequence, 86% less energy was consumed during the BioD-300 due to the avoidance of a  
609 solvent recovery unit, indicating here a major perspective to improve the energy balance of the  
610 microalgae-based biofuels process.

611 Other biorefinery approximations like the concomitant wastewater biorefinery [7–9], the zero-  
612 waste microalgal biorefinery [106] or multiple value-added biorefinery [107] have also identified  
613 similar bottlenecks in the production processes like harvesting efficiency, hybrid technologies and  
614 intensification, water consumption and culture productivity. The here proposed energy-driven

615 biorefinery approach may give some additional insights for retrieving and saving energy in other  
616 production processes where the use of a solvent-free metabolite recovery, the surplus of photovoltaic  
617 energy, and high biomass concentration processes, may be well integrated.

## 618 **4 Conclusions**

619 The here presented cumulative-improvement simulations have suggested that technologies such as  
620 intensified photobioreactors (thinner than 1-3 cm), infrared light filtering units, photovoltaic panels,  
621 solvent-free metabolite recovery processes such as decantation, and high biomass concentration  
622 treatments at  $\geq 145 \text{ kg}\cdot\text{m}^{-3}$  are major contributors on the net energy ratio of microalgae-based  
623 biofuel process. The conclusion was found consistent for both ideal and actual strains. These  
624 operations were also found to be key to the design of a sustainable microalgae-based biofuel process  
625 and also probably well integrated into other biorefinery approaches

## 626 **Acknowledgements**

627 VH acknowledges the National Council on Science and Technology (CONACyT, Mexico) for his  
628 research fellowship.

## 629 **Funding**

630 This research did not receive any specific grant from funding agencies in the public, commercial,  
631 or not-for-profit sectors.

632 **References**

- 633 [1] Alalwan HA, Alminshid AH, Aljaafari HA. Promising evolution of biofuel generations. Subject  
634 review. *Renewable Energy Focus* 2019;28(March):127–39. doi:10.1016/j.ref.2018.12.006.
- 635 [2] Shuba ES, Kifle D. Microalgae to biofuels: ‘Promising’ alternative and renewable energy,  
636 review. *Renewable and Sustainable Energy Reviews* 2018;81(August 2017):743–55. doi:10.  
637 1016/j.rser.2017.08.042.
- 638 [3] Chisti Y. Biodiesel from microalgae. *Biotechnology Advances* 2007;25(3):294–306. doi:10.  
639 1016/j.biotechadv.2007.02.001.
- 640 [4] Chisti Y. Biodiesel from microalgae beats bioethanol. *Trends in Biotechnology*  
641 2008;26(3):126–31. doi:10.1016/j.tibtech.2007.12.002.
- 642 [5] Lakshmikandan M, Murugesan A, Wang S, Abomohra AEF, Jovita PA, Kiruthiga S. Sustain-  
643 able biomass production under CO<sub>2</sub> conditions and effective wet microalgae lipid extraction  
644 for biodiesel production. *Journal of Cleaner Production* 2020;247:119398. doi:10.1016/j.  
645 jclepro.2019.119398.
- 646 [6] Peng L, Fu D, Chu H, Wang Z, Qi H. Biofuel production from microalgae: a review. *Envi-  
647 ronmental Chemistry Letters* 2020;18(2):285–97. doi:10.1007/s10311-019-00939-0.
- 648 [7] Thangam KR, Santhiya A, Sri SA, MubarakAli D, Karthikumar S, Kumar RS, et al. Bio-  
649 refinery approaches based concomitant microalgal biofuel production and wastewater treat-  
650 ment. *Science of The Total Environment* 2021;785:147267. doi:10.1016/j.scitotenv.2021.  
651 147267.
- 652 [8] Bhatia SK, Mehariya S, Bhatia RK, Kumar M, Pugazhendhi A, Awasthi MK, et al. Wastew-  
653 ater based microalgal biorefinery for bioenergy production: Progress and challenges. *Science  
654 of The Total Environment* 2021;751:141599. doi:10.1016/j.scitotenv.2020.141599.
- 655 [9] Baldev E, Mubarak Ali D, Pugazhendhi A, Thajuddin N. Wastewater as an economical and  
656 ecofriendly green medium for microalgal biofuel production. *Fuel* 2021;294:120484. doi:10.  
657 1016/j.fuel.2021.120484.
- 658 [10] Khoo KS, Chew KW, Yew GY, Leong WH, Chai YH, Show PL, et al. Recent advances  
659 in downstream processing of microalgae lipid recovery for biofuel production. *Bioresource  
660 Technology* 2020;304:122996. doi:10.1016/j.biortech.2020.122996.

- 661 [11] Ponton JW. Biofuels: Thermodynamic sense and nonsense. *Journal of Cleaner Production*  
662 2009;17(10):896–9. doi:10.1016/j.jclepro.2009.02.003.
- 663 [12] Collet P, Lardon L, Hélias A, Bricout S, Lombaert-Valot I, Perrier B, et al. Biodiesel from mi-  
664 croalgae - Life cycle assessment and recommendations for potential improvements. *Renewable*  
665 *Energy* 2014;71:525–33. doi:10.1016/j.renene.2014.06.009.
- 666 [13] Moutel B, Gonçalves O, Le Grand F, Long M, Soudant P, Legrand J, et al. Development  
667 of a screening procedure for the characterization of *Botryococcus braunii* strains for biofuel  
668 application. *Process Biochemistry* 2016;51(11):1855–65. doi:10.1016/j.procbio.2016.05.  
669 002.
- 670 [14] Taleb A, Kandilian R, Touchard R, Montalescot V, Rinaldi T, Taha S, et al. Screening of  
671 freshwater and seawater microalgae strains in fully controlled photobioreactors for biodiesel  
672 production. *Bioresource Technology* 2016;218:480–90. doi:10.1016/j.biortech.2016.06.  
673 086.
- 674 [15] Taleb A, Pruvost J, Legrand J, Marec H, Le-Gouic B, Mirabella B, et al. Development and  
675 validation of a screening procedure of microalgae for biodiesel production: Application to the  
676 genus of marine microalgae *Nannochloropsis*. *Bioresource Technology* 2015;177(January):224–  
677 32. doi:10.1016/j.biortech.2014.11.068.
- 678 [16] Benvenuti G, Bosma R, Cuaresma M, Janssen M, Barbosa MJ, Wijffels RH. Selecting mi-  
679 croalgae with high lipid productivity and photosynthetic activity under nitrogen starvation.  
680 *Journal of Applied Phycology* 2015;27(4):1425–31. doi:10.1007/s10811-014-0470-8.
- 681 [17] Ma Y, Wang Z, Yu C, Yin Y, Zhou G. Evaluation of the potential of 9 *Nannochloropsis*  
682 strains for biodiesel production. *Bioresource Technology* 2014;167:503–9. doi:10.1016/j.  
683 *biortech*.2014.06.047.
- 684 [18] Song M, Pei H, Hu W, Ma G. Evaluation of the potential of 10 microalgal strains for  
685 biodiesel production. *Bioresource Technology* 2013;141:245–51. doi:10.1016/j.biortech.  
686 2013.02.024.
- 687 [19] Heredia V, Gonçalves O, Marchal L, Pruvost J. Producing Energy-Rich Microalgae  
688 Biomass for Liquid Biofuels: Influence of Strain Selection and Culture Conditions. *Ener-*  
689 *gies* 2021;14(5):1246. doi:10.3390/en14051246.
- 690 [20] Kandilian R, Taleb A, Heredia V, Cogne G, Pruvost J. Effect of light absorption rate and  
691 nitrate concentration on TAG accumulation and productivity of *Parachlorella kessleri* cultures

- 692 grown in chemostat mode. *Algal Research* 2019;39(October 2018):101442. doi:10.1016/j.  
693 *algal*.2019.101442.
- 694 [21] Simionato D, Block MA, La Rocca N, Jouhet J, Maréchal E, Finazzi G, et al. The response  
695 of *Nannochloropsis gaditana* to nitrogen starvation includes de novo biosynthesis of triacyl-  
696 glycerols, a decrease of chloroplast galactolipids, and reorganization of the photosynthetic  
697 apparatus. *Eukaryotic Cell* 2013;12(5):665–76. doi:10.1128/EC.00363–12.
- 698 [22] Janssen JH, Lamers PP, de Vos RC, Wijffels RH, Barbosa MJ. Translocation and de novo  
699 synthesis of eicosapentaenoic acid (EPA) during nitrogen starvation in *Nannochloropsis gadi-*  
700 *tana*. *Algal Research* 2019;37(November 2018):138–44. doi:10.1016/j.*algal*.2018.11.025.
- 701 [23] Lee E, Pruvost J, He X, Munipalli R, Pilon L. Design tool and guidelines for outdoor  
702 photobioreactors. *Chemical Engineering Science* 2014;106:18–29. doi:10.1016/j.*ces*.2013.  
703 11.014.
- 704 [24] Pruvost J, Cornet JF, Le Borgne F, Goetz V, Legrand J. Theoretical investigation of microal-  
705 gae culture in the light changing conditions of solar photobioreactor production and compari-  
706 son with cyanobacteria. *Algal Research* 2015;10:87–99. doi:10.1016/j.*algal*.2015.04.005.
- 707 [25] Reay D, Ramshaw C, Harvey A. *Process Intensification*. Elsevier; 2008. ISBN 9780750689410.  
708 doi:10.1016/B978-0-7506-8941-0.X0001-6.
- 709 [26] Pruvost J, Le Borgne F, Artu A, Legrand J. Development of a thin-film solar photobioreactor  
710 with high biomass volumetric productivity (AlgoFilm©) based on process intensification  
711 principles. *Algal Research* 2017;21:120–37. doi:10.1016/j.*algal*.2016.10.012.
- 712 [27] Legrand J. *ADVANCES IN CHEMICAL ENGINEERING Photobioreaction Engineering*.  
713 In: *Journal of Chemical Information and Modeling*; vol. 43. ISBN 9788578110796; 2013, p.  
714 1689–99.
- 715 [28] Nwoba EG, Parlevliet DA, Laird DW, Alameh K, Louveau J, Pruvost J, et al. Energy  
716 efficiency analysis of outdoor standalone photovoltaic-powered photobioreactors coproducing  
717 lipid-rich algal biomass and electricity. *Applied Energy* 2020;275(March):115403. doi:10.  
718 1016/j.*apenergy*.2020.115403.
- 719 [29] Faried M, Samer M, Abdelsalam E, Yousef RS, Attia YA, Ali AS. Biodiesel production from  
720 microalgae: Processes, technologies and recent advancements. *Renewable and Sustainable*  
721 *Energy Reviews* 2017;79(May):893–913. doi:10.1016/j.*rser*.2017.05.199.

- 722 [30] Halim R, Danquah MK, Webley PA. Extraction of oil from microalgae for biodiesel produc-  
723 tion: A review. *Biotechnology Advances* 2012;30(3):709–32. doi:10.1016/j.biotechadv.  
724 2012.01.001.
- 725 [31] Yuan J, Kendall A, Zhang Y. Mass balance and life cycle assessment of biodiesel from  
726 microalgae incorporated with nutrient recycling options and technology uncertainties. *GCB*  
727 *Bioenergy* 2015;7(6):1245–59. doi:10.1111/gcbb.12229.
- 728 [32] Günerken E, D’Hondt E, Eppink MH, Garcia-Gonzalez L, Elst K, Wijffels RH. Cell disruption  
729 for microalgae biorefineries. *Biotechnology Advances* 2015;33(2):243–60. doi:10.1016/j.  
730 biotechadv.2015.01.008.
- 731 [33] Safi C, Cabas Rodriguez L, Mulder WJ, Engelen-Smit N, Spekking W, van den Broek LA,  
732 et al. Energy consumption and water-soluble protein release by cell wall disruption of *Nan-*  
733 *nochloropsis gaditana*. *Bioresource Technology* 2017;239:204–10. doi:10.1016/j.biortech.  
734 2017.05.012.
- 735 [34] Lee SJ, Yoon BD, Oh HM. Rapid method for the determination of lipid from the green alga  
736 *Botryococcus braunii*. *Biotechnology Techniques* 1998;12:553–6. doi:doi.org/10.1023/A:  
737 1008811716448.
- 738 [35] Montalescot V, Rinaldi T, Touchard R, Jubeau S, Frappart M, Jaouen P, et al. Optimization  
739 of bead milling parameters for the cell disruption of microalgae: Process modeling and ap-  
740 plication to *Porphyridium cruentum* and *Nannochloropsis oculata*. *Bioresource Technology*  
741 2015;196:339–46. doi:10.1016/j.biortech.2015.07.075.
- 742 [36] Zinkoné TR, Gifuni I, Lavenant L, Pruvost J, Marchal L. Bead milling disruption kinet-  
743 ics of microalgae: Process modeling, optimization and application to biomolecules recovery  
744 from *Chlorella sorokiniana*. *Bioresource Technology* 2018;267(July):458–65. doi:10.1016/j.  
745 biortech.2018.07.080.
- 746 [37] Postma PR, Suarez-Garcia E, Safi C, Olivieri G, Olivieri G, Wijffels RH, et al. Energy efficient  
747 bead milling of microalgae: Effect of bead size on disintegration and release of proteins and  
748 carbohydrates. *Bioresource Technology* 2017;224:670–9. doi:10.1016/j.biortech.2016.11.  
749 071.
- 750 [38] Sati H, Mitra M, Mishra S, Baredar P. Microalgal lipid extraction strategies for biodiesel  
751 production: A review. *Algal Research* 2019;38(January):101413. doi:10.1016/j.algal.  
752 2019.101413.

- 753 [39] Balasubramanian RK, Yen Doan TT, Obbard JP. Factors affecting cellular lipid extraction  
754 from marine microalgae. *Chemical Engineering Journal* 2013;215-216:929–36. doi:10.1016/  
755 j.cej.2012.11.063.
- 756 [40] Harris J, Viner K, Champagne P, Jessop PG. Advances in microalgal lipid extraction for  
757 biofuel production: a review. *Biofuels, Bioproducts and Biorefining* 2018;12(6):1118–35.  
758 doi:10.1002/bbb.1923.
- 759 [41] Seyfang B, Klein A, Grützner T. Extraction Centrifuges—Intensified Equipment Facilitat-  
760 ing Modular and Flexible Plant Concepts. *ChemEngineering* 2019;3(1):17. doi:10.3390/  
761 chemengineering3010017.
- 762 [42] Bojczuk M, Żyzelewicz D, Hodurek P. Centrifugal partition chromatography – A review of re-  
763 cent applications and some classic references. *Journal of Separation Science* 2017;40(7):1597–  
764 609. doi:10.1002/jssc.201601221.
- 765 [43] Ungureanu C, Marchal L, Chirvase AA, Foucault A. Centrifugal partition extraction, a  
766 new method for direct metabolites recovery from culture broth: Case study of torularhodin  
767 recovery from *Rhodotorula rubra*. *Bioresource Technology* 2013;132:406–9. doi:10.1016/j.  
768 biortech.2012.11.105.
- 769 [44] Heredia V, Pruvost J, Gonçalves O, Drouin D, Marchal L. Lipid recovery from *Nan-*  
770 *nochloropsis gaditana* using the wet pathway: Investigation of the operating parame-  
771 ters of bead milling and centrifugal extraction. *Algal Research* 2021;56(February):102318.  
772 doi:10.1016/j.algal.2021.102318.
- 773 [45] Angles E, Jaouen P, Pruvost J, Marchal L. Wet lipid extraction from the microalga *Nan-*  
774 *nochloropsis* sp.: Disruption, physiological effects and solvent screening. *Algal Research*  
775 2017;21:27–34. doi:10.1016/j.algal.2016.11.005.
- 776 [46] Gifuni I, Pollio A, Safi C, Marzocchella A, Olivieri G. Current Bottlenecks and Challenges  
777 of the Microalgal Biorefinery. *Trends in Biotechnology* 2019;37(3):242–52. doi:10.1016/j.  
778 tibtech.2018.09.006.
- 779 [47] Chew KW, Yap JY, Show PL, Suan NH, Juan JC, Ling TC, et al. Microalgae biorefinery:  
780 High value products perspectives. *Bioresource Technology* 2017;229:53–62. doi:10.1016/j.  
781 biortech.2017.01.006.
- 782 [48] Suganya T, Varman M, Masjuki HH, Renganathan S. Macroalgae and microalgae as a po-  
783 tential source for commercial applications along with biofuels production: A biorefinery ap-

- 784 proach. *Renewable and Sustainable Energy Reviews* 2016;55:909–41. doi:10.1016/j.rser.  
785 2015.11.026.
- 786 [49] Mendoza A, Morales V, Sanchez-Bayo A, Rodriguez-Escudero R, Gonzalez-Fernandez C,  
787 Bautista LF, et al. The effect of the lipid extraction method used in biodiesel produc-  
788 tion on the integrated recovery of biodiesel and biogas from *Nannochloropsis gaditana*,  
789 *Isochrysis galbana* and *Arthrospira platensis*. *Biochemical Engineering Journal* 2020;154(July  
790 2019):107428. doi:10.1016/j.bej.2019.107428.
- 791 [50] Posada JA, Brentner LB, Ramirez A, Patel MK. Conceptual design of sustainable integrated  
792 microalgae biorefineries: Parametric analysis of energy use, greenhouse gas emissions and  
793 techno-economics. *Algal Research* 2016;17:113–31. doi:10.1016/j.algal.2016.04.022.
- 794 [51] Venkata Subhash G, Rajvanshi M, Raja Krishna Kumar G, Shankar Sagaram U, Prasad V,  
795 Govindachary S, et al. Challenges in microalgal biofuel production: A perspective on techno  
796 economic feasibility under biorefinery stratagem. *Bioresource Technology* 2022;343:126155.  
797 doi:10.1016/j.biortech.2021.126155.
- 798 [52] Rajesh Banu J, Preethi , Kavitha S, Gunasekaran M, Kumar G. Microalgae based biore-  
799 finery promoting circular bioeconomy-techno economic and life-cycle analysis. *Bioresource*  
800 *Technology* 2020;302:122822. doi:10.1016/j.biortech.2020.122822.
- 801 [53] Sander K, Murthy GS. Life cycle analysis of algae biodiesel. *International Journal of Life*  
802 *Cycle Assessment* 2010;15(7):704–14. doi:10.1007/s11367-010-0194-1.
- 803 [54] Borowitzka Ma, Moheimani NR. *Algae for Biofuels and Energy*. Dordrecht: Springer Nether-  
804 lands; 2013. ISBN 978-94-007-5478-2. doi:10.1007/978-94-007-5479-9.
- 805 [55] Harun R, Danquah MK, Forde GM. Microalgal biomass as a fermentation feedstock for  
806 bioethanol production. *Journal of Chemical Technology and Biotechnology* 2009;85(2):199–  
807 203. doi:10.1002/jctb.2287.
- 808 [56] Karemore A, Sen R. Downstream processing of microalgal feedstock for lipid and carbohy-  
809 drate in a biorefinery concept: a holistic approach for biofuel applications. *RSC Advances*  
810 2016;6(35):29486–96. doi:10.1039/C6RA01477A.
- 811 [57] Sivaramakrishnan R, Incharoensakdi A. Utilization of microalgae feedstock for concomitant  
812 production of bioethanol and biodiesel. *Fuel* 2018;217(December 2017):458–66. doi:10.1016/  
813 j.fuel.2017.12.119.

- 814 [58] Hossain N, Zaini J, Indra Mahlia TM. Life cycle assessment, energy balance and sensitivity  
815 analysis of bioethanol production from microalgae in a tropical country. *Renewable and*  
816 *Sustainable Energy Reviews* 2019;115(April):109371. doi:10.1016/j.rser.2019.109371.
- 817 [59] Weissman JC, Goebel RP, Benemann JR. Photobioreactor design: Mixing, carbon utilization,  
818 and oxygen accumulation. *Biotechnology and Bioengineering* 1988;31(4):336–44. doi:10.  
819 1002/bit.260310409.
- 820 [60] Chiaramonti D, Prussi M, Casini D, Tredici MR, Rodolfi L, Bassi N, et al. Review of energy  
821 balance in raceway ponds for microalgae cultivation: Re-thinking a traditional system is  
822 possible. *Applied Energy* 2013;102:101–11. doi:10.1016/j.apenergy.2012.07.040.
- 823 [61] Tredici MR, Bassi N, Prussi M, Biondi N, Rodolfi L, Chini Zittelli G, et al. Energy balance of  
824 algal biomass production in a 1-ha "Green Wall Panel" plant: How to produce algal biomass  
825 in a closed reactor achieving a high Net Energy Ratio. *Applied Energy* 2015;154:1103–11.  
826 doi:10.1016/j.apenergy.2015.01.086.
- 827 [62] Souliès A, Pruvost J, Legrand J, Castelain C, Burghelea TI. Rheological properties of sus-  
828 pensions of the green microalga *Chlorella vulgaris* at various volume fractions. *Rheologica*  
829 *Acta* 2013;52(6):589–605. doi:10.1007/s00397-013-0700-z.
- 830 [63] Delrue F, Setier PA, Sahut C, Cournac L, Roubaud A, Peltier G, et al. An economic,  
831 sustainability, and energetic model of biodiesel production from microalgae. *Bioresource*  
832 *Technology* 2012;111:191–200. doi:10.1016/j.biortech.2012.02.020.
- 833 [64] Zhang H, Zhang X. Microalgal harvesting using foam flotation: A critical review. *Biomass*  
834 *and Bioenergy* 2019;120(October 2018):176–88. doi:10.1016/j.biombioe.2018.11.018.
- 835 [65] Xu K, Zou X, Chang W, Qu Y, Li Y. Microalgae harvesting technique using ballasted  
836 flotation: A review. *Separation and Purification Technology* 2021;276(July):119439. doi:10.  
837 1016/j.seppur.2021.119439.
- 838 [66] Zinkoné TR. Broyage à billes de microalgues : étude et modélisation par classe de taille,  
839 application au bioraffinage. Ph.D. thesis; Université de Nantes; 2018. URL: [http://www.](http://www.theses.fr/2018NANT4084)  
840 [theses.fr/2018NANT4084](http://www.theses.fr/2018NANT4084).
- 841 [67] Kim S, Chen J, Cheng T, Gindulyte A, He J, He S, et al. PubChem 2019 update: improved  
842 access to chemical data. *Nucleic Acids Research* 2019;47(D1):D1102–9. doi:10.1093/nar/  
843 gky1033.

- 844 [68] Miao X, Wu Q. High yield bio-oil production from fast pyrolysis by metabolic controlling  
845 of *Chlorella protothecoides*. *Journal of Biotechnology* 2004;110(1):85–93. doi:10.1016/j.  
846 jbiotec.2004.01.013.
- 847 [69] Sicaire AG, Vian MA, Filly A, Li Y, Bily A, Chemat F. 2-Methyltetrahydrofuran: Main  
848 Properties, Production Processes, and Application in Extraction of Natural Products. July.  
849 ISBN 9783662436288; 2014, p. 253–68. doi:10.1007/978-3-662-43628-8\_12.
- 850 [70] Pashchenko LL, Kuznetsova TS. The enthalpies of vaporization of some hydrocarbons with  
851 three-membered rings. *Russian Journal of Physical Chemistry A* 2007;81(11):1738–42. doi:10.  
852 1134/S0036024407110040.
- 853 [71] Fukuda H, Kondo A, Noda H. Biodiesel fuel production by transesterification of oils. *Journal*  
854 *of Bioscience and Bioengineering* 2001;92(5):405–16. doi:10.1016/S1389-1723(01)80288-7.
- 855 [72] Batan L, Quinn J, Willson B, Bradley T. Net energy and greenhouse gas emission evaluation of  
856 biodiesel derived from microalgae. *Environmental Science and Technology* 2010;44(20):7975–  
857 80. doi:10.1021/es102052y.
- 858 [73] Lee TH, Kim MY, Ryu YW, Seo JH. Estimation of theoretical yield for ethanol production  
859 from D-xylose by recombinant *Saccharomyces cerevisiae* using a metabolic pathway synthesis  
860 algorithm. *Journal of Microbiology and Biotechnology* 2001;11(3):384–8.
- 861 [74] Okamoto K, Uchii A, Kanawaku R, Yanase H. Bioconversion of xylose, hexoses and biomass  
862 to ethanol by a new isolate of the white rot basidiomycete *Trametes versicolor*. *SpringerPlus*  
863 2014;3(1):1–9. doi:10.1186/2193-1801-3-121.
- 864 [75] Tibbetts SM, Milley JE, Lall SP. Chemical composition and nutritional properties of freshwa-  
865 ter and marine microalgal biomass cultured in photobioreactors. *Journal of Applied Phycology*  
866 2015;27(3):1109–19. doi:10.1007/s10811-014-0428-x.
- 867 [76] Xu H, Miao X, Wu Q. High quality biodiesel production from a microalga *Chlorella protothe-*  
868 *coides* by heterotrophic growth in fermenters. *Journal of Biotechnology* 2006;126(4):499–507.  
869 doi:10.1016/j.jbiotec.2006.05.002.
- 870 [77] Khuong LS, Zulkifli NW, Masjuki HH, Mohamad EN, Arslan A, Mosarof MH, et al. A review  
871 on the effect of bioethanol dilution on the properties and performance of automotive lubricants  
872 in gasoline engines. *RSC Advances* 2016;6(71):66847–69. doi:10.1039/c6ra10003a.

- 873 [78] Pérez-López P, de Vree JH, Feijoo G, Bosma R, Barbosa MJ, Moreira MT, et al. Comparative  
874 life cycle assessment of real pilot reactors for microalgae cultivation in different seasons.  
875 Applied Energy 2017;205:1151–64. doi:10.1016/j.apenergy.2017.08.102.
- 876 [79] Slade R, Bauen A. Micro-algae cultivation for biofuels: Cost, energy balance, environmen-  
877 tal impacts and future prospects. Biomass and Bioenergy 2013;53:29–38. doi:10.1016/j.  
878 biombioe.2012.12.019.
- 879 [80] Pruvost J, Goetz V, Artu A, Das P, Al Jabri H. Thermal modeling and optimization of  
880 microalgal biomass production in the harsh desert conditions of State of Qatar. Algal Research  
881 2019;38(December 2018):101381. doi:10.1016/j.algal.2018.12.006.
- 882 [81] Pruvost J, Le Gouic B, Lepine O, Legrand J, Le Borgne F. Microalgae culture in building-  
883 integrated photobioreactors: Biomass production modelling and energetic analysis. Chemical  
884 Engineering Journal 2016;284:850–61. doi:10.1016/j.cej.2015.08.118.
- 885 [82] Benemann JR, Oswald WJ. Systems and Economic Analysis of Microalgae Ponds for Con-  
886 version of CO<sub>2</sub> to Biomass. Tech. Rep.; Pittsburgh Energy Technology Center, U.S. Dept. of  
887 Energy; 1996. URL: [https://digital.library.unt.edu/ark:/67531/metadc680796/m2/  
888 1/high\\_res\\_d/493389.pdf](https://digital.library.unt.edu/ark:/67531/metadc680796/m2/1/high_res_d/493389.pdf).
- 889 [83] Lehr F, Posten C. Closed photo-bioreactors as tools for biofuel production. Current Opinion  
890 in Biotechnology 2009;20(3):280–5. doi:10.1016/j.copbio.2009.04.004.
- 891 [84] Norsker NH, Barbosa MJ, Vermuë MH, Wijffels RH. Microalgal production — A close look at  
892 the economics. Biotechnology Advances 2011;29(1):24–7. doi:10.1016/j.biotechadv.2010.  
893 08.005.
- 894 [85] Hadiyanto H, Elmore S, Van Gerven T, Stankiewicz A. Hydrodynamic evaluations in high  
895 rate algae pond (HRAP) design. Chemical Engineering Journal 2013;217:231–9. doi:10.1016/  
896 j.cej.2012.12.015.
- 897 [86] Liffman K, Paterson DA, Liovic P, Bandopadhyay P. Comparing the energy efficiency of  
898 different high rate algal raceway pond designs using computational fluid dynamics. Chemical  
899 Engineering Research and Design 2013;91(2):221–6. doi:10.1016/j.cherd.2012.08.007.
- 900 [87] Pruvost J, Le Borgne F, Artu A, Cornet JF, Legrand J. Industrial Photobioreactors and  
901 Scale-Up Concepts. In: Advances in Chemical Engineering: Photobioreaction Engineering.  
902 Elsevier; 2016, p. 257–310. doi:10.1016/bs.ache.2015.11.002.

- 903 [88] Illman A, Scragg A, Shales S. Increase in *Chlorella* strains calorific values when grown in  
904 low nitrogen medium. *Enzyme and Microbial Technology* 2000;27(8):631–5. doi:10.1016/  
905 S0141-0229(00)00266-0.
- 906 [89] Goetz V, Le Borgne F, Pruvost J, Plantard G, Legrand J. A generic temperature model for  
907 solar photobioreactors. *Chemical Engineering Journal* 2011;175:443–9. doi:10.1016/j.cej.  
908 2011.09.052.
- 909 [90] de Farias Silva CE, Bertucco A. Bioethanol from microalgae and cyanobacteria: A review and  
910 technological outlook. *Process Biochemistry* 2016;51(11):1833–42. doi:10.1016/j.procbio.  
911 2016.02.016.
- 912 [91] Ho SH, Huang SW, Chen CY, Hasunuma T, Kondo A, Chang JS. Bioethanol production using  
913 carbohydrate-rich microalgae biomass as feedstock. *Bioresource Technology* 2013;135:191–8.  
914 doi:10.1016/j.biortech.2012.10.015.
- 915 [92] Klinke HB, Thomsen AB, Ahring BK. Inhibition of ethanol-producing yeast and bacteria by  
916 degradation products produced during pre-treatment of biomass. *Applied Microbiology and  
917 Biotechnology* 2004;66(1):10–26. doi:10.1007/s00253-004-1642-2.
- 918 [93] Wei P, Cheng LH, Zhang L, Xu XH, Chen HL, Gao CJ. A review of membrane technology  
919 for bioethanol production. *Renewable and Sustainable Energy Reviews* 2014;30:388–400.  
920 doi:10.1016/j.rser.2013.10.017.
- 921 [94] Lewandowicz G, Białas W, Marczewski B, Szymanowska D. Application of membrane dis-  
922 tillation for ethanol recovery during fuel ethanol production. *Journal of Membrane Science*  
923 2011;375(1-2):212–9. doi:10.1016/j.memsci.2011.03.045.
- 924 [95] Brennan L, Owende P. Biofuels from microalgae-A review of technologies for production,  
925 processing, and extractions of biofuels and co-products. *Renewable and Sustainable Energy  
926 Reviews* 2010;14(2):557–77. doi:10.1016/j.rser.2009.10.009.
- 927 [96] Vitova M, Bisova K, Kawano S, Zachleder V. Accumulation of energy reserves in algae:  
928 From cell cycles to biotechnological applications. *Biotechnology Advances* 2014;33(6):1204–  
929 18. doi:10.1016/j.biotechadv.2015.04.012.
- 930 [97] Adhikari S, Fernando SD, Haryanto A. Hydrogen production from glycerol: An update.  
931 *Energy Conversion and Management* 2009;50(10):2600–4. doi:10.1016/j.enconman.2009.  
932 06.011.

- 933 [98] Postma P, Miron T, Olivieri G, Barbosa M, Wijffels R, Eppink M. Mild disintegration of the  
934 green microalgae *Chlorella vulgaris* using bead milling. *Bioresource Technology* 2015;184:297–  
935 304. doi:10.1016/j.biortech.2014.09.033.
- 936 [99] Doucha J, Lívanský K. Influence of processing parameters on disintegration of *Chlorella* cells  
937 in various types of homogenizers. *Applied Microbiology and Biotechnology* 2008;81(3):431–40.  
938 doi:10.1007/s00253-008-1660-6.
- 939 [100] Marchal L, Legrand J, Foucault A. Mass transport and flow regimes in centrifugal partition  
940 chromatography. *AIChE Journal* 2002;48(8):1692–704. doi:10.1002/aic.690480811.
- 941 [101] Togarcheti SC, kumar Mediboyina M, Chauhan VS, Mukherji S, Ravi S, Mudliar SN,  
942 et al. Life cycle assessment of microalgae based biodiesel production to evaluate the im-  
943 pact of biomass productivity and energy source. *Resources, Conservation and Recycling*  
944 2017;122:286–94. doi:10.1016/j.resconrec.2017.01.008.
- 945 [102] Kim DG, La HJ, Ahn CY, Park YH, Oh HM. Harvest of *Scenedesmus* sp. with bioflocculant  
946 and reuse of culture medium for subsequent high-density cultures. *Bioresource Technology*  
947 2011;102(3):3163–8. doi:10.1016/j.biortech.2010.10.108.
- 948 [103] Wang S, Yerkebulan M, Abomohra AEF, El-Khodary S, Wang Q. Microalgae harvest  
949 influences the energy recovery: A case study on chemical flocculation of *Scenedesmus*  
950 *obliquus* for biodiesel and crude bio-oil production. *Bioresource Technology* 2019;286:121371.  
951 doi:10.1016/j.biortech.2019.121371.
- 952 [104] Lakshmikandan M, Wang S, Murugesan A, Saravanakumar M, Selvakumar G. Co-cultivation  
953 of *Streptomyces* and microalgal cells as an efficient system for biodiesel production and biofloc-  
954 culation formation. *Bioresource Technology* 2021;332:125118. doi:10.1016/j.biortech.  
955 2021.125118.
- 956 [105] Pugazhendhi A, Nagappan S, Bhosale RR, Tsai PC, Natarajan S, Devendran S, et al. Var-  
957 ious potential techniques to reduce the water footprint of microalgal biomass production  
958 for biofuel—A review. *Science of The Total Environment* 2020;749:142218. doi:10.1016/j.  
959 scitotenv.2020.142218.
- 960 [106] Mishra S, Roy M, Mohanty K. Microalgal bioenergy production under zero-waste biorefinery  
961 approach: Recent advances and future perspectives. *Bioresource Technology* 2019;292:122008.  
962 doi:10.1016/j.biortech.2019.122008.

- 963 [107] Bhattacharya M, Goswami S. Microalgae – A green multi-product biorefinery for future  
964 industrial prospects. *Biocatalysis and Agricultural Biotechnology* 2020;25:101580. doi:10.  
965 1016/j.bcab.2020.101580.

966 **Authorship contribution statement**

967 **Vladimir Heredia:** Conceptualization, Formal analysis, Investigation, Writing - Original Draft.

968 **Jeremy Pruvost:** Conceptualization, Writing - Review & Editing, Supervision. **Jack Legrand:**

969 Supervision.

970 **Declaration of interests**

971 The authors declare that they have no known competing financial interests or personal relationships

972 that could have appeared to influence the work reported in this paper.